Neuron
Article

Sez-6 Proteins Affect Dendritic Arborization Patterns and Excitability of Cortical Pyramidal Neurons

Jenny M. Gunnersen,[1,3,*] Mary H. Kim,[1,3] Stephanie J. Fuller,[1] Melanie De Silva,[1] Joanne M. Britto,[1] Vicki E. Hammond,[1] Philip J. Davies,[1] Steve Petrou,[1] E.S. Louise Faber,[2] Pankaj Sah,[2] and Seong-Seng Tan[1,*]
[1]Brain Development Laboratory, Howard Florey Institute, The University of Melbourne, Parkville, Victoria, 3010, Australia
[2]The Queensland Brain Institute, University of Queensland, St Lucia, Queensland, 4072, Australia
[3]These two authors contributed equally to this work.
*Correspondence: jenny.gunnersen@florey.edu.au (J.M.G.), stan@florey.edu.au (S.-S.T.)
DOI 10.1016/j.neuron.2007.09.018

SUMMARY

Development of appropriate dendritic arbors is crucial for neuronal information transfer. We show, using seizure-related gene 6 (*sez-6*) null mutant mice, that Sez-6 is required for normal dendritic arborization of cortical neurons. Deep-layer pyramidal neurons in the somatosensory cortex of *sez-6* null mice exhibit an excess of short dendrites, and cultured cortical neurons lacking Sez-6 display excessive neurite branching. Overexpression of individual Sez-6 isoforms in knockout neurons reveals opposing actions of membrane-bound and secreted Sez-6 proteins, with membrane-bound Sez-6 exerting an antibranching effect under both basal and depolarizing conditions. Layer V pyramidal neurons in knockout brain slices show reduced excitatory postsynaptic responses and a reduced dendritic spine density, reflected by diminished punctate staining for postsynaptic density 95 (PSD-95). In behavioral tests, the *sez-6* null mice display specific exploratory, motor, and cognitive deficits. In conclusion, cell-surface protein complexes involving Sez-6 help to sculpt the dendritic arbor, in turn enhancing synaptic connectivity.

INTRODUCTION

The ability of neurons to receive and integrate synaptic information depends to an extent on their dendritic morphology. Certain dendritic arborization patterns established during development are characteristic of particular neuronal subtypes and relate to function (Häusser et al., 2000; Wong and Ghosh, 2002). The basic dendritic scaffold is likely to be specified, at least partially, by molecular programs intrinsic to the neuron (Moore et al., 2002; Sugimura et al., 2004), although the initial orientation (Polleux et al., 2000) and subsequent elaboration of dendritic branches are also influenced by extrinsic signals and afferent activity. Many factors have been shown to influence dendritic growth and branching of cortical neurons. Such agents include brain-derived neurotrophic factor and other neurotrophins (McAllister et al., 1995), epidermal growth factor (Goldshmit et al., 2004), hepatocyte growth factor (Gutierrez et al., 2004), and insulin-like growth factor (Niblock et al., 2000), all of which increase dendritic complexity. Similarly, Slit, together with its receptor, Roundabout (Whitford et al., 2002), and Semaphorin 3A, via its coreceptors neuropilin1 and plexinA1 (Fenstermaker et al., 2004), both induce dendritic growth and branching, while Notch mediates contact-dependent inhibition of dendritic outgrowth while stimulating branching (Sestan et al., 1999).

The process of dendritic growth in the developing brain is known to be highly dynamic, with extension and retraction of filopodia and stabilization or elimination of dendritic branches occurring over time frames of minutes to hours (Wu et al., 1999). The question of how partnerships between innervating afferent axons and dendritic branches are first established and then maintained at an appropriate level to effectively cover the target area has been widely studied (Wong and Ghosh, 2002; Vaughn, 1989; Niell et al., 2004). The "synaptotropic hypothesis" of dendritic growth and branching posits that dendritic branching patterns are modulated by initial synaptic contacts such that the complexity of the mature arbor correlates with the number of afferent terminals in the synaptogenic field (Vaughn, 1989). In support of this, synapse formation on dendritic filopodia correlated with stabilization and maturation of the filopodium into a dendritic branch in the zebrafish optic tectum (Niell et al., 2004). Similarly, individual dendritic branches of chick retinal neurons were stabilized by neurotransmitter-evoked local calcium release (Lohmann et al., 2002), indicating the importance of neuronal activity in dendritic arbor morphogenesis (Wong and Ghosh, 2002; Haas et al., 2006).

In the mature brain, dendritic patterning is maintained by physiological levels of afferent activity (Tailby et al., 2005; Chklovskii et al., 2004), although dendritic spines

are subject to turnover (Trachtenberg et al., 2002). Changes in spine density in vivo have been associated with altered afferent activity resulting from experimental manipulation or disease. For example, monocular impulse blockade during the critical period reduced apical dendrite spine number by 26% (Riccio and Matthews, 1985), and epilepsy (Swann et al., 2000), schizophrenia (Glantz and Lewis, 2000), and Down's syndrome (Suetsugu and Mehraein, 1980) are likewise characterized by regional reductions in dendritic spine number.

Seizure-related gene 6 (*sez-6*) is an activity-regulated mRNA transcript, found to be acutely upregulated in cortical neurons treated with the convulsant drug, pentylenetetrazole (PTZ) (Shimizu-Nishikawa et al., 1995). Previously, linkage between *sez-6* and known epilepsy- or PTZ-susceptibility loci was not found (Wakana et al., 2000), although recently an association between *sez-6* mutation and febrile seizure has been reported (Yu et al., 2007). *Sez-6* mRNA levels are elevated in the cortex during prenatal development (Gunnersen et al., 2002; Kim et al., 2002) and after having been trained in an enriched environment (Rampon et al., 2000). A recent study reported NMDA receptor-dependent elevation of *sez-6* mRNA levels in the hippocampal dentate gyrus after long-term potentiation induction (Håvik et al., 2007), suggesting Sez-6 involvement in the activity-dependent plasticity of learning and memory.

The *sez-6* gene encodes three isoforms, of which two (Sez-6 type I [tI] and type II [tII]) are cell-surface proteins tethered by a single transmembrane domain. A secreted isoform, Sez-6 type III (tIII), arises from an alternatively spliced mRNA transcript to produce a truncated protein identical to the amino terminal sequences of tI and tII except for 18 C-terminal amino acids. All predicted Sez-6 protein isoforms contain the known protein-protein interaction domains, CUB (complement subcomponent C1r, C1s/sea urchin embryonic growth factor Uegf/bone morphogenetic protein 1) and SCR (short consensus repeat). The presence of these domains implies that the function of Sez-6 proteins involves binding to other extracellular or cell-surface proteins. Recently, Sez-6 has been reported to bind neurotrypsin (S. Mitsui et al., 2006, Soc. Neurosci, abstract), a serine protease mutated in autosomal recessive nonsyndromic mental retardation (Molinari et al., 2002) and shown to be required for long-term memory in *Drosophila* (Didelot et al., 2006). Other CUB domain-containing type I transmembrane proteins have been found to regulate acetylcholine receptor clustering (Gally et al., 2004) and gating of ionotropic glutamate receptors (Zheng et al., 2004) in *C. elegans*. The CUB domain-containing neuropilins mediate the effects of Semaphorins, including guiding migrating neurons (Marín et al., 2001), patterning dendrites (Fenstermaker et al., 2004), and modulating synaptic transmission (Sahay et al., 2005). Taken together, the structural domains and expression pattern of Sez-6 suggested possible roles in neuronal development and function.

This study was conducted to understand the functional role of Sez-6, particularly in regard to dendritic patterning and synaptic regulation. We report that cortical neurons of mice lacking all Sez-6 isoforms show altered dendritic arborization. In the absence of Sez-6, increased dendritic branching of cortical neurons is observed; however, the excess branches are short, interstitial branches that do not increase dendritic field area. We demonstrate that the secreted and membrane-bound isoforms of Sez-6 exert opposite actions whereby the secreted isoform increases, and the membrane-bound isoform decreases, neurite number. Furthermore, branching induced by chronic KCl depolarization is counteracted by overexpression of membrane-bound Sez-6 in knockout (KO) neurons. Pyramidal cortical neurons lacking Sez-6 show attenuated excitatory synaptic transmission relative to control neurons, which is primarily a consequence of having fewer excitatory synapses. In behavioral tests, the Sez-6 null mice display reduced exploratory behavior and motor coordination, altered maze performance, and poorer memory retention. From these results we conclude that Sez-6 acts at the cell surface to sculpt the dendritic arbor and influence synaptic connectivity.

RESULTS

Sez-6 Is Expressed in the Developing and Postnatal Mouse Forebrain

In order to study the cellular and tissue distribution of Sez-6 protein expression, we raised antibodies to purified, recombinant Sez-6 tIII. Protein expression patterns obtained using this anti-Sez-6 polyclonal antiserum (recognizing both secreted and membrane-bound isoforms; Figures S1A and S1B in the Supplemental Data available with this article online) closely matched the mRNA expression profile (Kim et al., 2002). Sez-6 is expressed strongly in postmitotic, maturing neurons of the developing cortical plate (cp) and subplate (sp) at embryonic day 13 (E13; Figure 1A) and E15 (Figures 1B and 1C and Figure S1C). Somewhat weaker expression is seen in the subpallial ganglionic eminences (cge, lge, mge; Figures 1A and 1B) and intermediate zone (iz, Figure 1B) and stronger, discrete expression domains are present in the thalamic eminences (te; Figure 1A). In the cortex, Sez-6 expression diminishes after birth although deep layer (layer V/VI) pyramidal neurons and neuronal subpopulations of layer II/III continue to express this protein (Figure 1D). In the hippocampus, Sez-6 expression persists in CA1 pyramidal neurons and in the dentate gyrus (dg; Figure 1D), where cells stained with Sez-6 in the hilus (hil) and subgranular zone (sgz) also express markers of developing neurons (Figures 1E and 1F). Subpopulations of adult cortical neurons expressing the interneuron markers calretinin and parvalbumin were positive for Sez-6 expression (Figure S2).

Inactivation of the *sez-6* Gene Increases Dendritic Branching of Cortical Neurons

At present, the function of Sez-6 is unknown, although the conserved structural features and developmentally restricted pattern of expression would predict that Sez-6

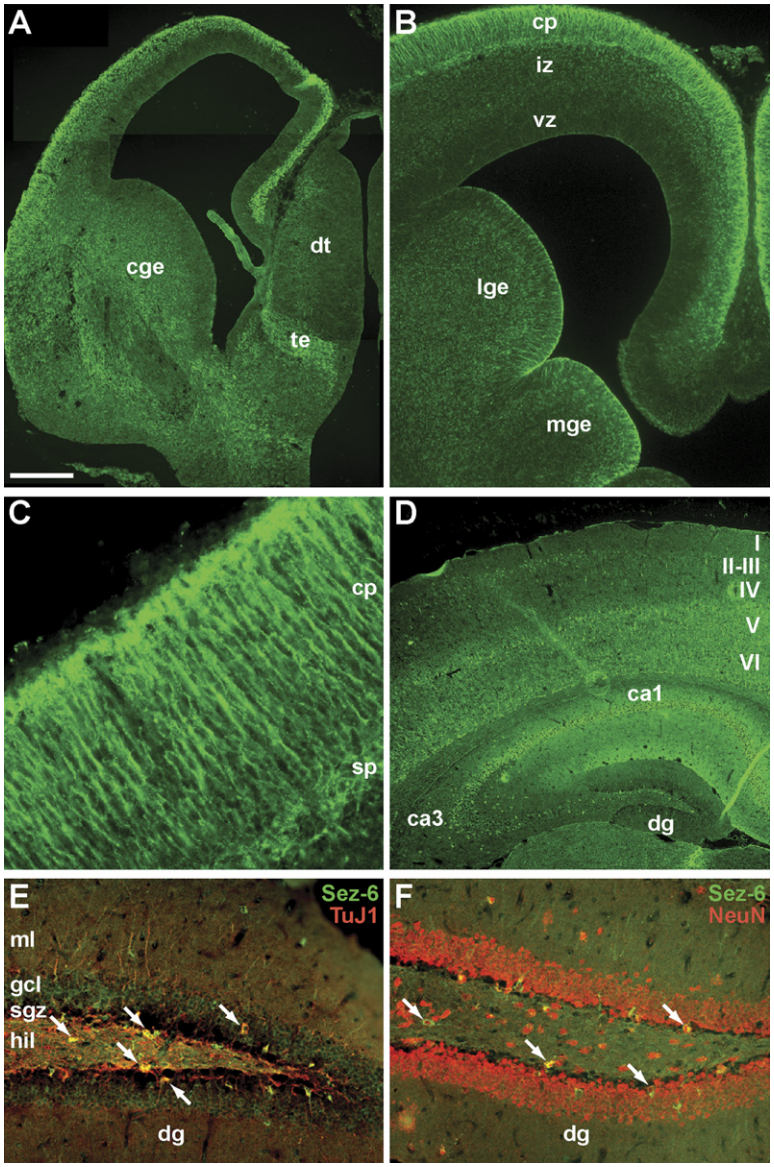

Figure 1. Expression of Sez-6 Proteins in the Developing and Mature Mouse Brain

Sez-6 expression in neurons of E13 (A) and E15 ([B and C], high power) embryonic brain. (D) Sez-6 expression at postnatal day 14 (P14) in cortex and hippocampus. (E) Double immunostaining for Sez-6 (green) and β-III-tubulin (red) in the adult hippocampal hilus and dentate gyrus. Double-stained neuronal precursors (yellow) are marked by arrows. (F) Neurons double-stained for Sez-6 and the neuronal nuclear marker NeuN (arrows) in the hilus and subgranular zone. Scale bar, 290 μm (A); 200 μm (B); 50 μm (C); 500 μm (D); 100 μm (E and F). ca1, ca3, *cornu ammonis* 1 or 3; cge, caudal ganglionic eminence; cp, cortical plate; dg, dentate gyrus; dt, dorsal thalamus; gcl, granule cell layer; hil, hilus; iz, intermediate zone; lge, lateral ganglionic eminence; mge, medial ganglionic eminence; ml, molecular layer; sgz, subgranular zone; sp, subplate; te, thalamic eminence; vz, ventricular zone; I–VI, cortical layers I–VI.

is important in cortical development. To investigate this, the *sez-6* gene was ablated by homologous recombination in embryonic stem cells. Transient Cre expression in homologous recombinant clones was then used to delete exon I (Figures 2A–2C; Supplemental Methods), removing transcriptional and translational initiation sites in the process. No Sez-6 protein was detected in null mutant mouse brain by immunohistochemistry (Figure 2D) or western blot (Figure 2E), confirming the functional inactivation of the *sez-6* gene. Sez-6 null mice were viable and fertile. They were born in the expected Mendelian ratio (33:50:26 for wild-type [WT], heterozygous, and homozygous null, respectively; n = 109), exhibited similar growth rates to WT littermates (data not shown), and displayed no obvious morphological abnormalities. In utero bromodeoxyuridine (BrdU) labeling of early-born (E12.5) and late-born (E15.5) cortical neurons revealed normal cortical layering (Figure S3A). Fluorogold injections into the brain stem to retrogradely label layer V revealed appropriate axonal projections and normal positioning of layer V neurons (Figure S3B).

We had demonstrated Sez-6 expression in maturing cortical neurons during the early postnatal period of dendritic arborization, leading us to postulate that Sez-6 might affect neurite outgrowth. To test this, embryonic neurons from KO E15.5 embryos and WT littermate controls were cultured at low density for 5 days in vitro (DIV), after which time neurons were immunostained for β-III tubulin and parameters of neurite growth and branching were analyzed. Cortical neurons isolated from Sez-6 null mutants displayed significantly greater neurite numbers (17.8 ± 1.0 and 25.6 ± 1.5 for WT and KO, respectively; $p < 0.05$), and this increase was observed for both primary and higher-order processes (Figures 3A and 3B). Interestingly, the

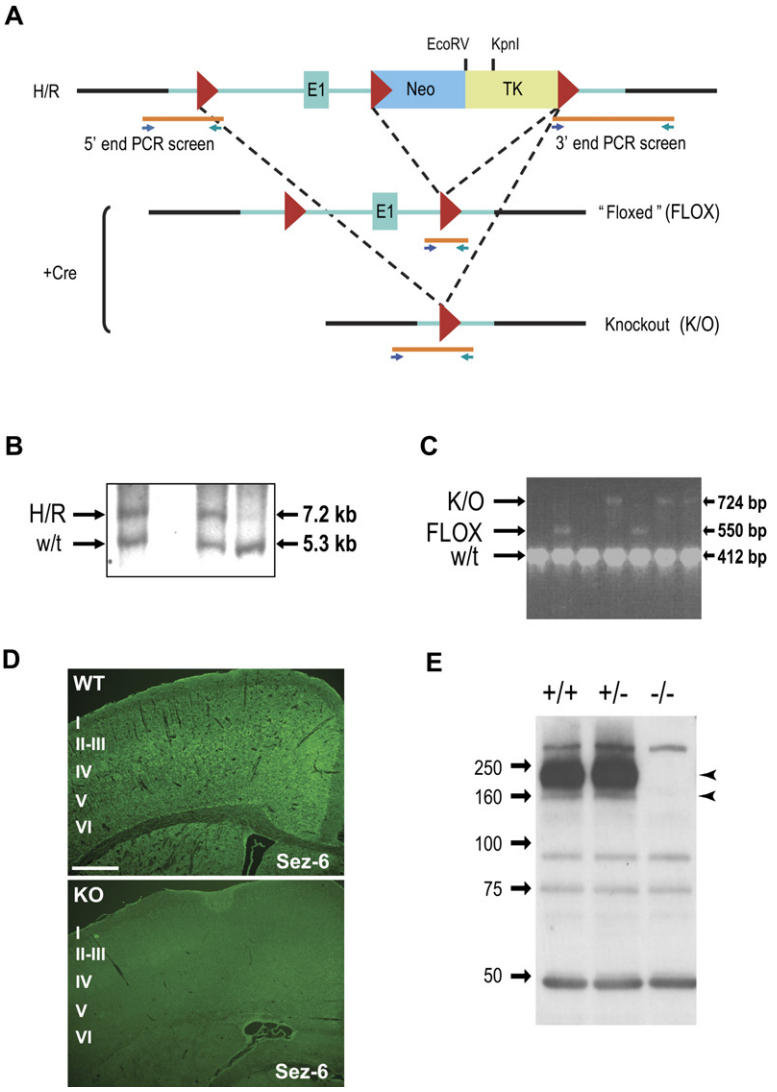

Figure 2. Generation of a *sez-6* Null Allele in Embryonic Stem Cells by Homologous Recombination Followed by Transient Cre Expression

(A) Exon I (E1) of the ~50 kb mouse *sez-6* gene flanked by loxP sites (red triangles) for Cre recombinase. Homologous recombinant (H/R) clones identified with the 5′PCR (forward primer site positioned upstream of the recombination site, as shown) were confirmed with an external 3′PCR reaction and Southern blot of EcoRV-digested genomic DNA (B) using an external probe. After Cre expression, floxed (FLOX), KO (K/O), and WT (w/t) alleles were simultaneously detected by multiplex PCR across loxP sites (A and C). (D) Sez-6 immunostaining of adult WT and Sez-6 KO coronal brain sections (scale bar, 500 μm). (E) Western blot of brain extracts from P16 WT (+/+), heterozygous (+/−), and KO (−/−) littermates. Specific Sez-6 bands are marked (arrowheads).

increased branching was found to correlate with a decrease in mean neurite length (Figure 3C) so that both the total neurite length (WT: 547.6 ± 29.5 μm, KO: 578.4 ± 33.8 μm) and dendritic field area (WT: 11359.6 ± 1214.5 μm^2; KO: 9378.9 ± 1105.5 μm^2) were unchanged.

Postnatally, Sez-6 expression remains high in specific cortical neuron populations, particularly those of the deep cortical layers. To determine whether the dendritic patterning of mature neurons was affected by the lack of Sez-6, we analyzed the dendritic arborization patterns of Golgi-Cox impregnated neurons in the somatosensory cortex. The cortex of Sez-6 null mutant mice appeared more heavily impregnated than that of WT (Figure 3D), and analysis of camera lucida images revealed that this effect was due, at least in part, to an increase in the number of dendritic branches per neuron. Layer V/VI pyramidal neurons of mutant mice exhibited more dendritic branching (Figure 3E). An increase in the number of tertiary branches (WT: 7.7 ± 0.9; KO: 11.1 ± 1.2; $p < 0.05$) and a similar trend for secondary branches was observed when dendritic traces from 30 neurons (from five brains) per genotype were compared (Figure 3F). To examine whether the branching phenotype is also manifest in lower-order dendrites, we scored layer V/VI neurons with pyramidal morphology for primary dendrites only. Neurons of Sez-6 null cortex had significantly more primary dendrites per neuron than those from WT cortex (WT: 5.2 ± 0.1; KO: 6.5 ± 0.17; $p < 0.001$; $n = 100$ per genotype, Figure 3G). Consistent with data from cultured neurons, the increase in branching had no net effect on the total dendritic length per cell measurement (WT: 825.7 ± 59.5 μm, KO: 874.0 ± 57.3 μm; $n = 30$).

Balanced Activity of Sez-6 Isoforms Determines Neurite Branching

Thus far, our results indicate that the net effect of removing all isoforms of Sez-6 is an increase in dendritic branching, although the KO mouse model does not permit the

actions of the secreted and membrane-bound Sez-6 isoforms to be analyzed independently. To investigate the respective roles of the secreted and membrane-bound isoforms, we conducted a series of experiments with dissociated neurons in vitro. First, we treated cortical neurons from WT embryos with Sez-6 tIII-conditioned medium. When WT neurons were exposed to exogenous Sez-6 tIII, they produced more neurites (tIII-treated: 22.9 ± 1.7, control: 17.1 ± 1.3; $p < 0.05$, $n = 68$, Figure 4A). The extra neurites were mainly higher-order branches (total neurites minus primary processes) and were predominantly short (<20 μm; Figure 4A). In other experiments, we cultured primary embryonic neurons on feeder layers exogenously secreting Sez-6 tIII. Under these conditions, KO neurons displayed more branches than WT neurons (WT: 12.2 ± 0.6; KO: 14.9 ± 0.8; $p < 0.05$, $n = 60$, Figure 4B) but, surprisingly, Sez-6 tIII secreted from feeder cells further enhanced 3° branches on Sez-6 KO neurons ($p < 0.05$, Figure 4C). To overexpress individual isoforms, we transfected Sez-6 KO neurons with expression constructs for tII, tIII, or control vector along with an EYFP reporter. Transfected KO neurons expressing high levels of ectopic Sez-6 tII (identified by Sez-6 immunofluorescence and EYFP fluorescence) displayed a decrease in neurite number ($p < 0.05$, Figure 4D), while tIII-expressing KO neurons showed a robust increase in this parameter ($p < 0.001$, Figure 4D), confirming the probranching effects of secreted Sez-6. Thus, Sez-6 can act on both WT and KO neurons, and furthermore, membrane-bound and secreted isoforms exert opposing actions.

Having demonstrated that overexpressed membrane-bound Sez-6 tII negatively influences dendritic arborization under basal conditions, we then investigated whether activity-dependent dendritic branching could be similarly affected. Dendritic branching induced by chronic depolarization with KCl has previously been shown to occur via calcium influx through voltage-gated calcium channels and altered nuclear signaling (Bading et al., 1993; Redmond et al., 2002). Treatment of Sez-6 KO neurons with KCl (50 mM for 24 hr from 3 DIV) enhanced dendritic branching (Figures 5A, 5B, and 5K), as previously reported for WT neurons. Sez-6 tII overexpression, on the other hand, resulted in reduced branching of both unstimulated (Figures 5C, 5E, 5F, and 5K) and KCl-stimulated neurons (Figures 3D and 3G–3K) relative to controls. In fact, in the presence of high Sez-6 tII levels, neurons depolarized by KCl showed a level of branching similar to untreated neurons and a generally stunted morphology (Figure 5D; cf. Figures 5C and 5K).

Neurons Lacking Sez-6 Show Reduced Excitatory Postsynaptic Potentials, or EPSPs

Since branching patterns are known to influence the integrative properties of dendritic arbors (Häusser et al., 2000), we assessed the impact of excessive branching on the electrical properties of Sez-6 KO neurons. Whole-cell recordings were made from layer V pyramidal neurons in the somatosensory cortex of litter-matched WT and KO Sez-6 mice. Most cells (31 of 32 cells from WT, and 23 of 30 cells from Sez-6 null mice) displayed firing properties similar to those of the "regular firing" class of layer V pyramidal neurons in rats (Williams and Stuart, 1999). The remaining WT neuron showed accommodation, while of the remaining Sez-6 null neurons, two showed accommodation, four were "weak burst firers," and one was a "strong burst firer" (Williams and Stuart, 1999). Neurons in both WT and Sez-6 null mice had similar electrotonic properties. WT and KO neurons had similar resting membrane potentials (−69.7 ± 1.2 mV and −65.1 ± 1.4 mV, respectively), input resistance (71.3 ± 5.0 MΩ and 66.1 ± 5.0 MΩ, respectively) and membrane time constants (18.1 ± 0.8 ms and 17.2 ± 0.7 ms, respectively). Moreover, no differences were found in the number of action potentials elicited by threshold depolarizing current injections (WT: 3.2 ± 0.3, $n = 32$; KO: 3.8 ± 0.3, $n = 30$), or the voltage threshold at which depolarizing current injection evoked an action potential (WT: −38.7 ± 0.6 mV, $n = 28$; KO: −38.9 ± 1.0 mV, $n = 23$). Thus, expression of voltage- and calcium-dependent ion channels is not altered in Sez-6 KO mice.

Increased dendritic branching of neurons in the KO cortex suggests possible functional differences in synaptic connections between layer II/III and layer V pyramidal cells. To examine inputs, we stimulated layer II/III, evoking a classical EPSP followed by a disynaptic inhibitory postsynaptic potential. In the Sez-6 KO neurons, the input-output curve of EPSPs was shifted to the right, whereby the EPSPs summated significantly less with increasing stimulus intensities compared with those in WT neurons (Figure 6A). Consequently, in WT neurons, increasing the stimulus intensity led to a gradually increasing EPSP that eventually reached threshold and generated action potentials in three out of five (60%) cells (Figure 6A). In contrast, EPSPs evoked with increasing stimulus intensity did not summate as well in KO neurons, and these summated EPSPs reached threshold in only one out of four (25%) cells, even with maximal (100V) stimulus intensities. In order to see whether this effect was due to the spike initiation threshold being shifted to more depolarized potentials in Sez-6 null neurons, the threshold of synaptically evoked action potentials was examined. In those cells that failed to fire an action potential with a single shock at maximal intensity, a train of five stimuli at 50 Hz was given to evoke firing. No difference in action potential threshold was found (WT: −41.8 ± 1.5 mV, $n = 8$; KO: −39.7 ± 1.9 mV, $n = 7$).

Stimulation in layer II/III will activate excitatory inputs to layer V pyramidal neurons and inhibitory inputs from local circuit interneurons. Thus, the reduction in EPSP summation may result either from a reduction in excitatory drive or an enhancement of GABAergic inhibition. We therefore examined synaptic summation in voltage-clamp (Vh = −50 mV), where the amplitude of both excitatory and inhibitory inputs could be monitored simultaneously. As with EPSPs, excitatory synaptic currents (EPSCs) summated significantly more with increasing stimulus

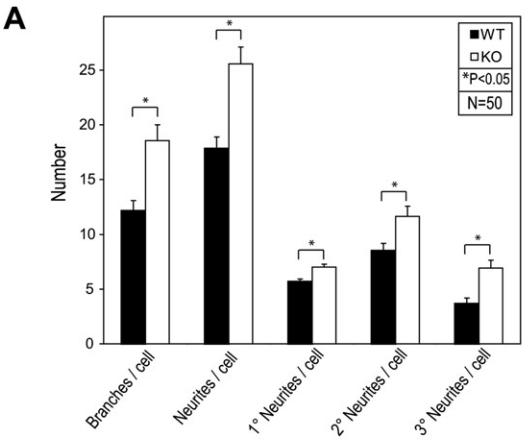
A
Number
WT
KO
*P<0.05
N=50
Branches / cell
Neurites / cell
1° Neurites / cell
2° Neurites / cell
3° Neurites / cell

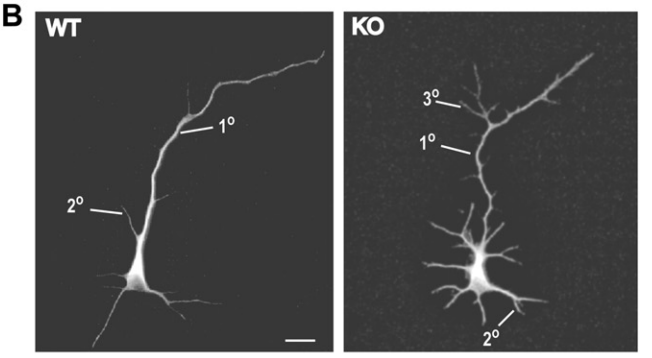
B
WT
KO
1°
2°
3°
1°
2°

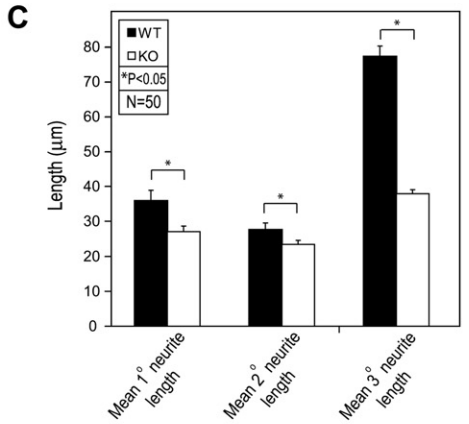
C
Length (µm)
WT
KO
*P<0.05
N=50
Mean 1° neurite length
Mean 2° neurite length
Mean 3° neurite length

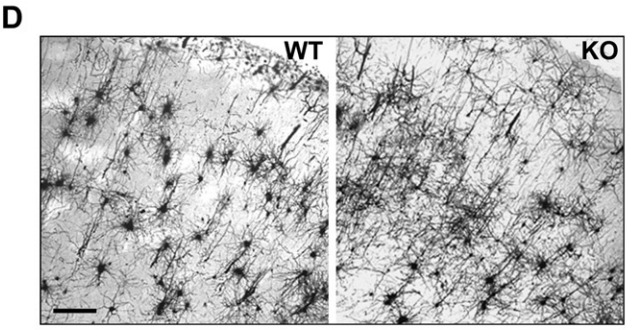
D
WT
KO

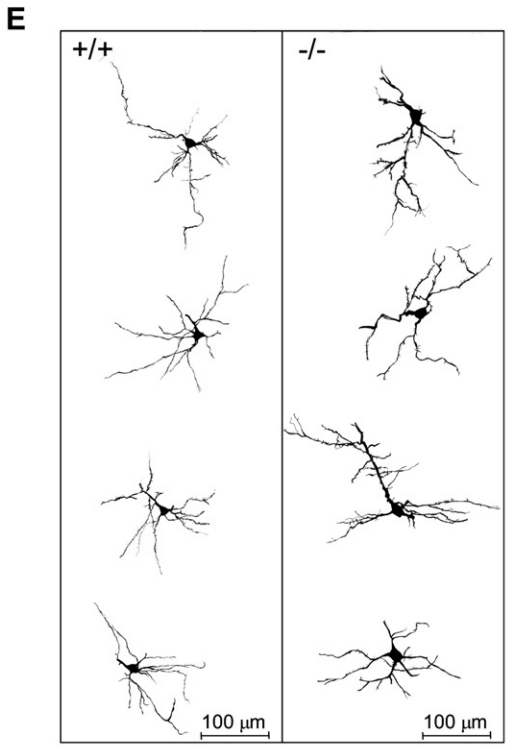
E
+/+
-/-
100 µm
100 µm

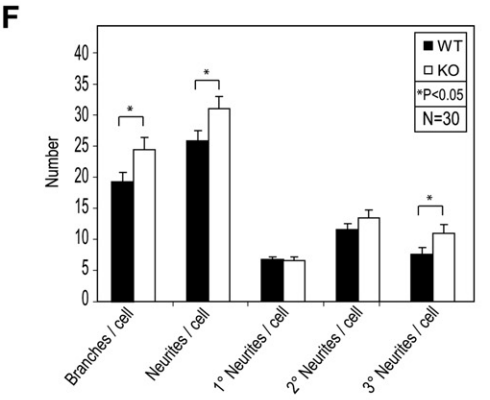
F
Number
WT
KO
*P<0.05
N=30
Branches / cell
Neurites / cell
1° Neurites / cell
2° Neurites / cell
3° Neurites / cell

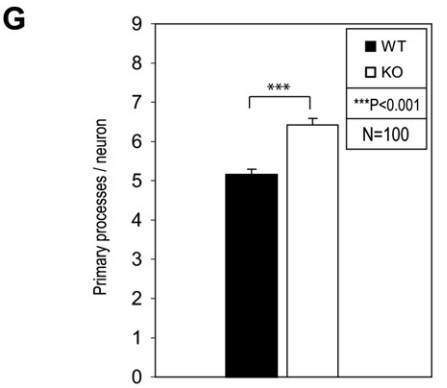
G
Primary processes / neuron
WT
KO
***P<0.001
N=100
***

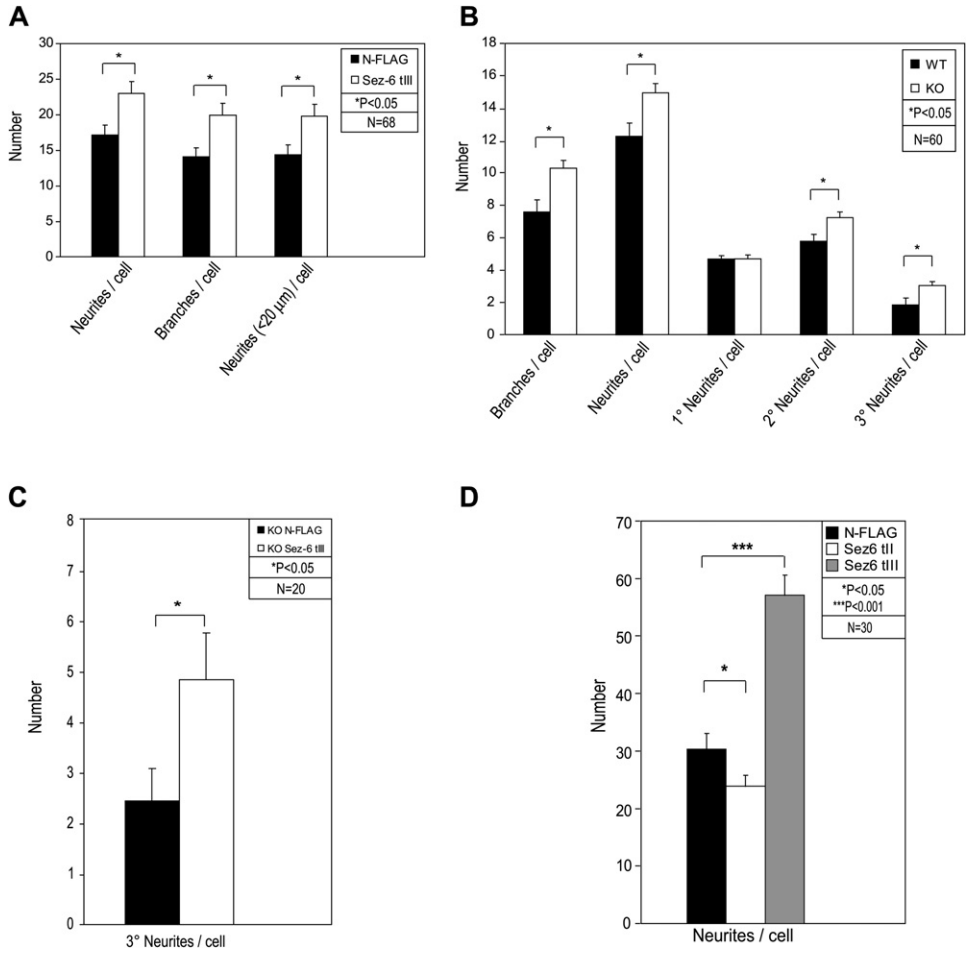

Figure 4. Exogenous Sez-6 Isoforms Alter Neurite/Branch Numbers on Neurons In Vitro

(A) Treatment of cultured neurons from E17.5 embryos with Sez-6 tIII-conditioned medium for 3 days increased neurite/branch numbers. The extra branches were predominantly short (<20 μm).

(B) E15.5 cortical neurons cultured on Cos-7 feeder layers (2–2.5 days) exhibited similar morphological parameters.

(C) KO neurons cultured on Sez-6 tIII-secreting feeder layers showed increased mean numbers of tertiary neurites compared with those of KO neurons on control feeder cells (N-FLAG vector).

(D) Cortical neurons from Sez-6 null mice expressing ectopic Sez-6 tII or tIII display significantly less or more neurites or filopodia, respectively, than controls (N-FLAG vector). Data are presented as mean ± SEM.

intensities in WT mice (n = 6) compared with the KOs (n = 4, Figure 6B). However, inhibitory postsynaptic currents (IPSCs) increased to a similar extent in the two sets of mice with increasing stimulus intensity (Figure 6B), suggesting that a reduction in excitatory drive rather than altered inhibitory drive contributes to the decreased synaptic efficacy in the Sez-6 null mice (see also Figure S4A). In agreement with this, no difference was found in the miniature IPSCs (mIPSCs) recorded in the presence of tetrodotoxin (TTX) (1 μM) between WT and KO mice, either in amplitude (WT: 40.9 ± 6.5 pA, n = 8; KO: 43.5 ± 8.5 pA, n = 7, $p > 0.05$) or frequency (WT: 13.5 ± 3.1 Hz, n = 8; KO: 12.0 ± 1.6 Hz, n = 7, $p > 0.05$, see Figures S4B–S4D). Together, these results indicate that there is a selective reduction in excitatory input to layer V pyramidal neurons in Sez-6 null mice. This

Figure 3. Primary Cultured Cortical Neurons from Sez-6 Null Embryos Display Increased Numbers of Short Neurites

(A) Compared to WT, KO cortical neurons exhibited more neurites (primary and higher-order). The number of branches was determined by subtraction of the number of primary dendrites from the total number of neurites. (B) Examples of TuJ1-stained neurons (scale bar, 20 μm). On average, neuritic processes in all categories were shorter in Sez-6 null cortex (C). (D) Golgi-Cox impregnated somatosensory cortex from WT and Sez-6 KO mice (scale bar, 200 μm). Deep-layer, KO cortical neurons in situ bore more branches than WT neurons; 3° dendrites predominated (examples of camera lucida tracings in [E]; n = 30 cells/genotype scored in [F]). (G) Numbers of 1° processes of deep-layer somatosensory pyramidal neurons were also significantly increased on KO neurons (n = 100 cells/genotype). Results are expressed as mean ± SEM.

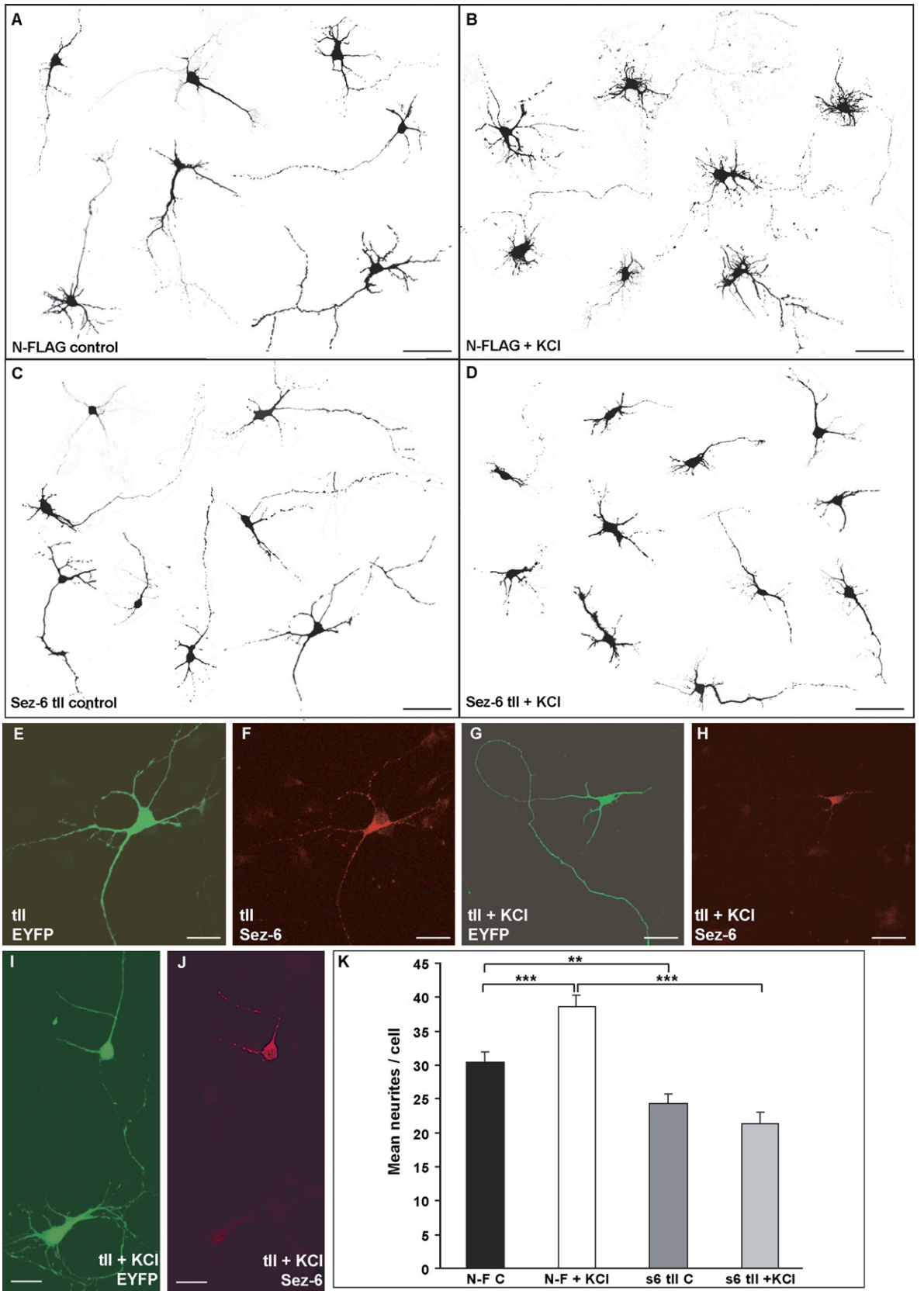
A
N-FLAG control
B
N-FLAG + KCl
C
Sez-6 tll control
D
Sez-6 tll + KCl
E
tll
EYFP
F
tll
Sez-6
G
tll + KCl
EYFP
H
tll + KCl
Sez-6
I
tll + KCl
EYFP
J
tll + KCl
Sez-6
K
Mean neurites / cell
45
40
35
30
25
20
15
10
5
0
**
***
***
N-F C
N-F + KCl
s6 tll C
s6 tll +KCl

reduction could be due either to a reduction in the number of connections to layer V neurons or to a reduction in the amplitude of unitary inputs. To distinguish between these alternatives, we first used minimal stimulation to activate putative single-fiber inputs (Raastad et al., 1992) and examined the EPSCs evoked. EPSCs evoked using minimal stimulation displayed clear failures (failure rate: 30% ± 4% in WT, n = 12; 29% ± 5% in KO, n = 11), confirming that they were single-fiber inputs. No significant difference in the mean amplitude of minimally stimulated EPSCs evoked in WT (31.4 ± 8.1 pA, n = 12) and Sez-6 null (23.8 ± 3 pA, n = 11, $p > 0.05$, Figure 6C) neurons was observed. In agreement with this result, no significant differences were observed in the amplitudes of miniature EPSCs (mEPSCs) examined in the presence of tetrodotoxin (1 μM). mEPSC amplitude was 30.7 ± 2.9 pA (n = 6) in WT mice compared with 35.9 ± 1.1 pA in KO mice (n = 5, $p > 0.05$, Figure 6D). These findings show that the reduced synaptic efficacy in the Sez-6 null mice results from a smaller number of functional connections between layer II/III and layer V pyramidal neurons, rather than changes in the potency of individual synaptic inputs.

Since Sez-6 was originally identified as a transcript upregulated by acute PTZ treatment of cortical neurons (Shimizu-Nishikawa et al., 1995) and since the altered electrophysiological properties of Sez-6 null neurons indicate fewer excitatory inputs, we constructed a dose-response curve to assess seizure susceptibility to PTZ in WT and Sez-6 KO mice (Figure S5). At higher doses of PTZ, Sez-6 mutant mice showed a trend toward a longer latency to tonic-clonic seizure involving hind limb extension, although a statistical comparison across all doses did not show significance (Figure S5B; $p > 0.05$). Nevertheless, a dose of 100 mg/kg PTZ induced a tonic-clonic seizure within the 1 hr observation period in six of nine WT mice while only one of six KO mice exhibited a maximal seizure (Fisher's exact test, $p = 0.078$).

Sez-6 Null Mice Display Reduced Dendritic Spine Density in Superficial Cortical Layers

To examine whether the number of excitatory synapses was altered in Sez-6 null mice, spine density on the apical dendritic branches of somatosensory layer V pyramidal neurons was determined in sections from Golgi-Cox impregnated brains (Figures 7A and 7B).

Spine density on dendrites projecting into cortical layer II/III was plotted as a function of the distance from the cell soma (Figure 7C). The density of dendritic spines on distal apical dendrites of layer V pyramidal neurons was found to be lower in Sez-6 KO somatosensory cortex than in control cortex (WT: 39.1 ± 3.0; KO: 29.7 ± 2.4; $p = 0.02$, Figure 7D). Similarly, we observed a reduced spine density and a greater proportion of spines exhibiting an immature morphology in cultured neurons (14 DIV) from Sez-6 null cortex relative to WT neurons plated at the same density (Figure S6). To investigate whether the reduced spine density on distal dendrites of layer V pyramidal neurons could result from a redistribution of afferent excitatory connections onto the supernumerary branches of Sez-6 null neurons, we measured the density of PSD-95 immunostained puncta in the neuropil of supragranular somatosensory cortex. Compared with WT, Sez-6 KO mice displayed a highly significant 28% reduction (WT: 19,519 ± 228 fluorescence intensity units; KO: 14,076 ± 278 fluorescence intensity units; Figures 7E and 7F) in mean staining intensity for this marker of the postsynaptic density in spine heads. In contrast, staining of adjacent sections for the dendritic marker microtubule-associated protein 2 (MAP-2) revealed that MAP-2 staining intensity was slightly increased in Sez-6 KO cortex relative to control (Figures 7E and 7F). The decreased density of PSD-95 puncta, in spite of an increase in MAP-2 staining, provides strong evidence for an overall reduction in, rather than a redistribution of, excitatory synapses on dendritic spines in cortical layers II/III of Sez-6 null mice.

Sez-6 Is Present on Dendrites and in the Postsynaptic Fraction But Is Not Strongly Associated with the Postsynaptic Density

We next examined the subcellular localization of Sez-6 to determine whether Sez-6 is present in spines and thus could be in a position to influence spine development or function directly. In both embryonic (Figures 8A–8C) and adult (Figures 8G–8L) cortical neurons, Sez-6 immunostaining colocalized with staining for the dendritic marker MAP-2, but not with nestin (E15; Figures 8D–8F) or the axon terminal synaptic vesicle marker synaptophysin (Figures 8M–8O). These results demonstrate that while Sez-6 expression is predominantly somatodendritic, it does not appear to be enriched at synapses, at least in the presynaptic axon terminal.

We examined this issue further by western blot analysis of subcellular fractions of WT mouse cortical protein extracts. The postsynaptic fractions were free of presynaptic vesicle membrane contamination as demonstrated by the absence of the 38 kDa synaptophysin band

Figure 5. Sez-6 tII Counteracts Activity-Dependent Dendritic Branching Stimulated by KCl Depolarization

(A) Sez-6 KO neurons cotransfected with the empty N-FLAG control vector and EYFP reporter plasmid. (B) Control KO neurons (N-FLAG and EYFP transfected) treated with 50 mM KCl. (C) Unstimulated KO neurons overexpressing Sez-6 tII. (D) Sez-6 tII-overexpressing KO neurons stimulated with 50 mM KCl. Transfected neurons were identified by EYFP fluorescence (E, G, and I) and Sez-6 tII overexpression was detected immunocytochemically (F, H, and J). Neurons expressing high levels of Sez-6 tII tended to have simpler dendritic arbors (I and J). Results are plotted as mean ± SEM neurite number per neuron (K). Data from two independent experiments were combined and duplicate coverslips for each condition were analyzed from each experiment (n = 61, 66, 61, and 70 for N-FLAG control, N-FLAG + KCl, tII control, and tII + KCl, respectively). ***$p < 0.001$, **$p < 0.005$. Scale bars, 50 μm (A–D); 20 μm (E–J).

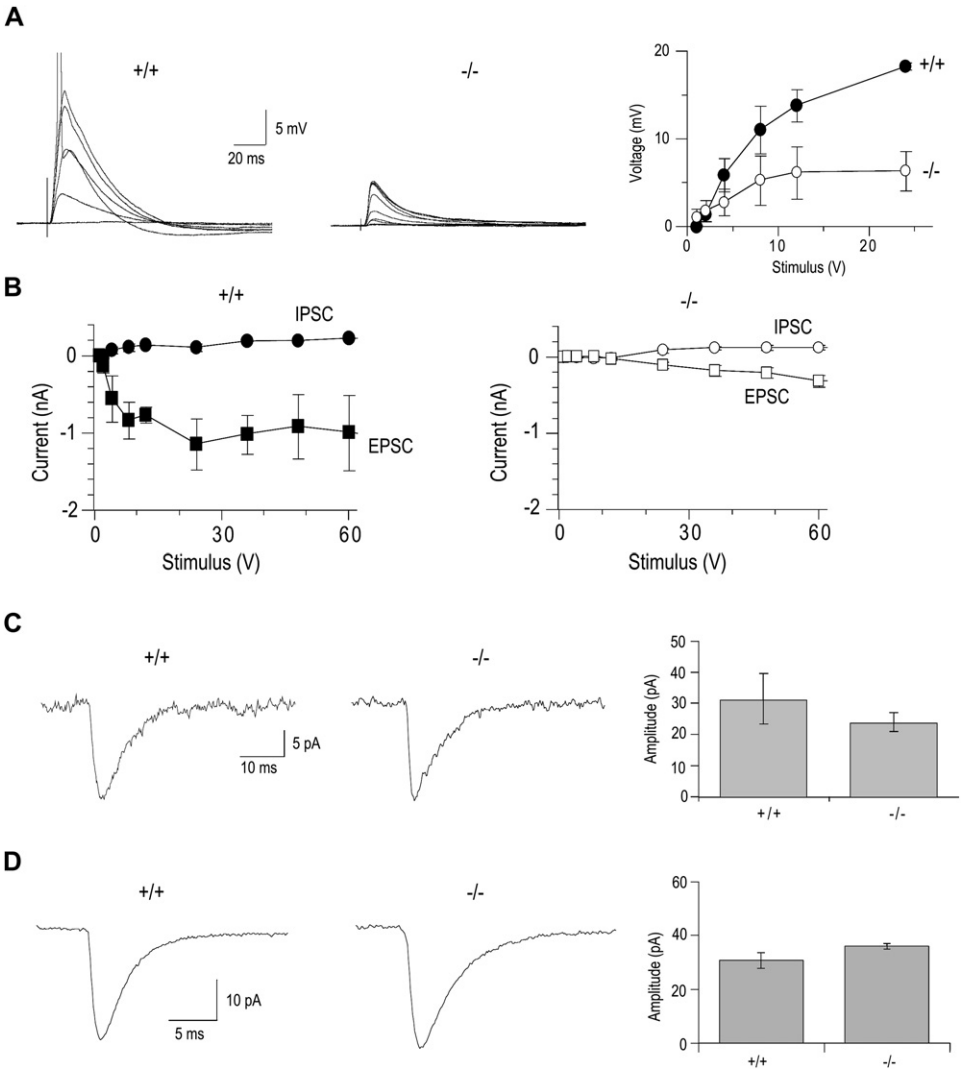

Figure 6. Excitatory Synaptic Connectivity between Layer II/III and Layer V Pyramidal Neurons Is Reduced in Sez-6 Null Mice

(A) Summating EPSPs (left) recorded in layer V pyramidal neurons evoked by synaptic stimulation in layer II/III. The EPSP increased in amplitude with larger stimulation and finally reached threshold and evoked an action potential (spike truncated for clarity) in WT (+/+) mice. In Sez-6 null (−/−) mice, increasing synaptic stimulation led to much smaller summation, and the EPSP did not reach threshold. Summary data (peak EPSP amplitude plotted against stimulus intensity) for *sez-6*$^{+/+}$ mice (n = 6) and *sez-6*$^{-/-}$ mice (n = 4) is shown to the right. The EPSP amplitude plateaus at a lower stimulus intensity in *sez-6*$^{-/-}$ mice.

(B) In voltage clamp (Vh = −50), the peak IPSC amplitude (circles) and peak EPSC amplitude (squares) have been plotted against stimulus intensity for *sez-6*$^{+/+}$ mice (left, filled symbols) and *sez-6*$^{-/-}$ mice (right, open symbols). Potency of inhibitory transmission is not affected in *sez-6*$^{-/-}$ mice.

(C) Representative EPSCs evoked by minimal stimulation in *sez-6*$^{+/+}$ (left trace) and *sez-6*$^{-/-}$ (middle trace) neurons are shown with summary histogram (right; n = 12 for *sez-6*$^{+/+}$ mice, n = 11 for *sez-6*$^{-/-}$ mice).

(D) Spontaneous miniature EPSCs recorded from a *sez-6*$^{+/+}$ animal (left trace) and a *sez-6*$^{-/-}$ animal (middle trace) are shown with a summary histogram (right; n = 6 for *sez-6*$^{+/+}$ mice, n = 5 for *sez-6*$^{-/-}$ mice).

(Figure 9). Specific Sez-6 bands were detected in all subcellular fractions with the exception of the detergent-insoluble postsynaptic fraction that was solubilized in 8M urea. The extrasynaptic fraction, containing proteins solubilized from presyaptic and postsynaptic extrajunctional plasma membrane and synaptic vesicles (Phillips et al., 2001), was relatively enriched for Sez-6. Since Sez-6 and synaptophysin exhibited nonoverlapping staining patterns (Figures 8M–8O), the source of the Sez-6 in the extrasynaptic membrane fraction is likely to be postsynaptic membrane, consistent with its localization along dendritic shafts (see Figures 8G–8L). Interestingly, Sez-6 is also present in the postsynaptic fraction (Figure 9) although, unlike PSD-95, it was completely extracted by strong detergent extraction (with 5% SDS) that presumably solubilizes residual

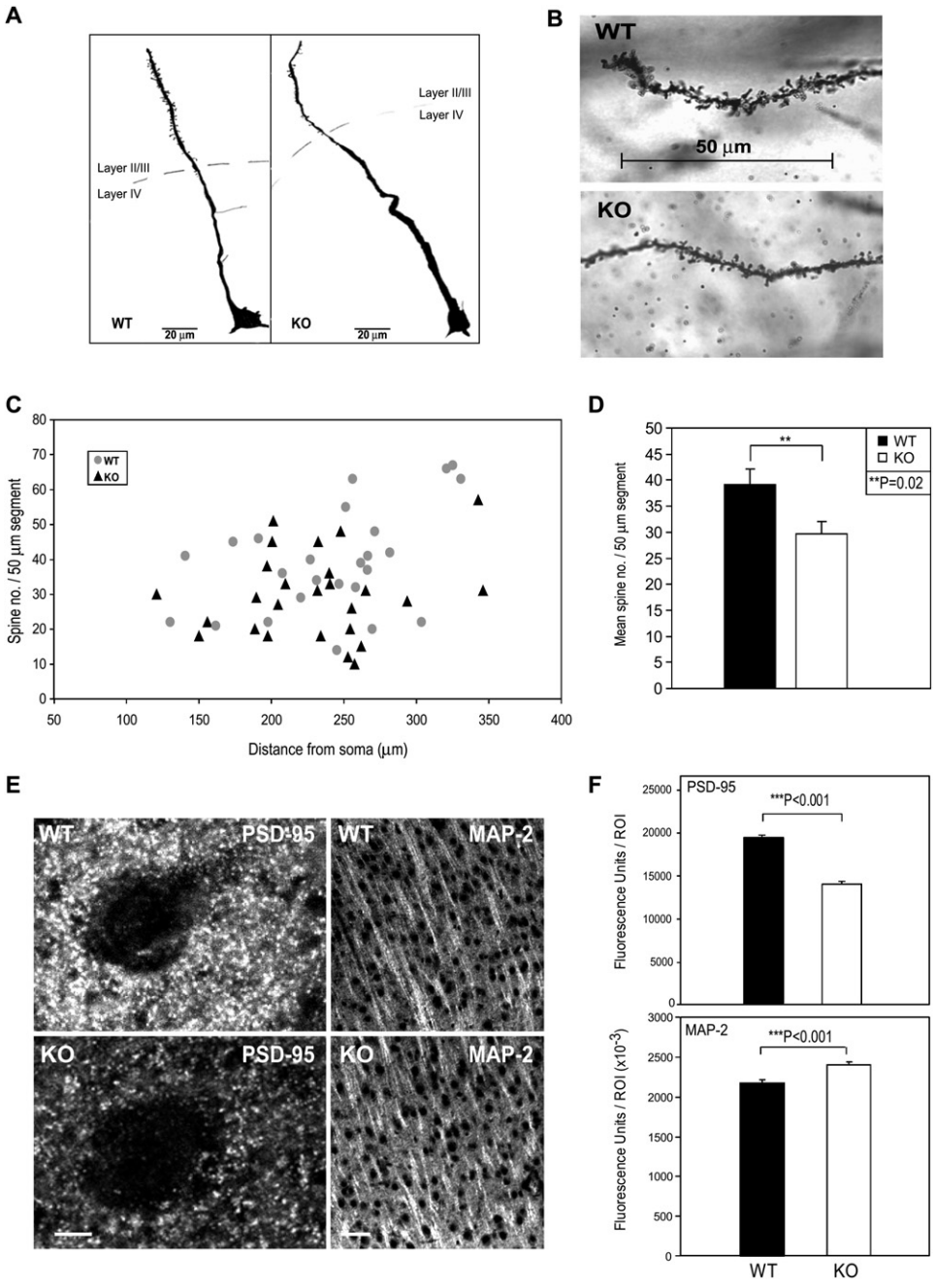

Figure 7. Sez-6 KO Neurons Show Reduced Spine Density on Apical Dendrites, which Correlates with a Reduction in PSD-95 Levels

(A) Camera lucida tracings of the apical dendrites of deep-layer pyramidal neurons in the somatosensory cortex of adult (5- to 7-week-old) mice.

(B) Distal segments of WT and KO layer V pyramidal neuron dendrites in layer II/III.

(C) Raw spine density data (n = 25 or 26 segments from 25 or 23 neurons for WT or KO brains, respectively) plotted against distance from soma.

(D) Mean spine density ± SEM (for all segments 100–400 μm from the soma) was significantly reduced on distal dendrites of Sez-6 null neurons.

(E) PSD-95 punctate immunostaining (left panels; scale bar, 10 μm) or MAP-2 immunostaining (right panels; scale bar, 50 μm) in layer II/III of somatosensory cortex.

(F) PSD-95 and MAP-2 immunostaining intensity plotted as mean (±SEM) pixel density/ROI.

membranes (resistant to the 1% Triton-X extraction) as well as proteins more loosely associated with the PSD. Thus, although Sez-6 is present in dendritic spines as well as dendritic shafts, any association with proteins of the PSD complex is disrupted by detergent extraction.

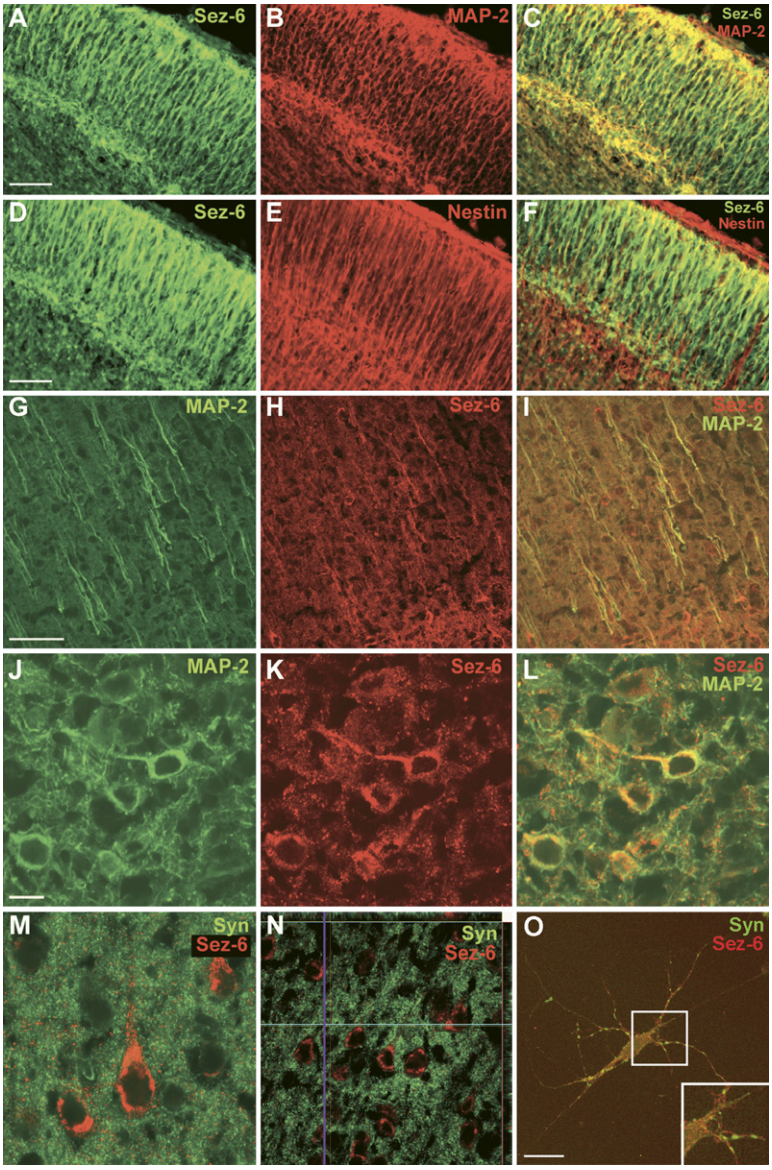

Figure 8. Sez-6 Colocalizes with the Dendritic Marker MAP-2, But Not with Axon Terminals Marked by Synaptophysin

(A–F) E15 cortex. Immunostaining for Sez-6 (A) and MAP-2 (B) partially overlap (C); however, no overlap is seen for Sez-6 (D) and nestin (E) in the merged image (F).

(G–N) Adult cortex. Apical dendrites (G–I), the neuronal soma, and primary dendrites (J–L) of deep-layer neurons double-stain for Sez-6 and MAP-2. (M and N) Punctate Sez-6 immunostaining along dendrites of layer V pyramidal neurons does not overlap with synaptophysin-positive puncta in the neuropil. In (N), linescan profiles are shown (upper and right sides of the main panel). (O) Embryonic hippocampal neuron in vitro (E18 + 6 DIV). Expression patterns of Sez-6 and synaptophysin are nonoverlapping.

Scale bar, 50 μm (A–I and N); 10 μm (J–M); 20 μm ([O]; inset, 12 μm).

Sez-6 Null Mice Display Motor Deficits and Altered Behavior in Maze Tests

Collectively, the molecular, morphological, and electrophysiological evidence of defects in dendritic arbor patterning and excitatory synaptic function in Sez-6 null mice prompted a comprehensive behavioral evaluation of these mice using a primary screen (described in Supplemental Methods). In all tests other than those described here, mice lacking Sez-6 were indistinguishable from age- and gender-matched WT controls, demonstrating that Sez-6 null mice are normal in many respects. In contrast, differences between WT and Sez-6 mutant mice were observed in tests of general activity, motor function, anxiety-related and depression-related behaviors, and spatial memory. In locomotor tests, mice lacking Sez-6 covered less distance (trials 2–5; Figure 10A) and were less prone to rearing behavior than controls (Figure 10B). Even though they were less active after habituation than WT controls, Sez-6 null mice displayed similar levels of activity in the horizontal plane during the first trial in the locomotor cell (Figure 10A). This exploratory response to a novel environment was also seen in the elevated plus maze (EPM) and Y-maze, where Sez-6 WT and KO mice exhibited no difference in the number of EPM or Y-maze arm entries (data not shown). In spite of this, Sez-6 KO mice showed behavioral differences in these tests, spending significantly more time than their WT counterparts on the open arms of the plus maze (Figure 10C) and in the novel arm of the Y-maze (Figure 10D). Mice lacking Sez-6 displayed reduced baseline immobility in the tail suspension test (Figure 10E) and a shorter latency to fall from the accelerating Rota-Rod,

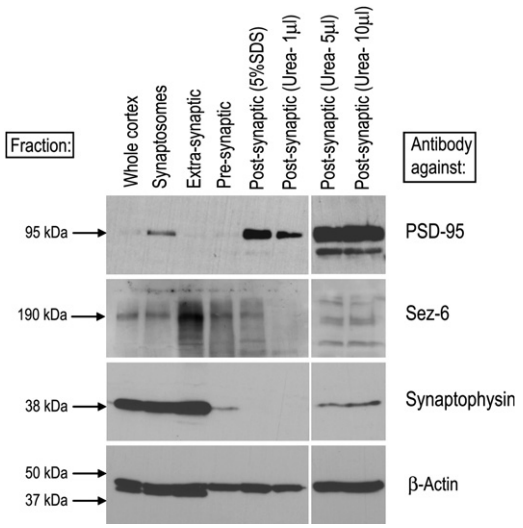

Figure 9. Sez-6 Is Distributed in Extrasynaptic and Synaptic Subcellular Fractions

Western blot of whole cortex extract and subcellular fractions from WT mouse brain (10 μg protein/lane, or indicated volume of urea-solubilized postsynaptic material from total 60 μl) probed for PSD-95, Sez-6, synaptophysin, or β-actin loading control.

with the mean latency being only ~70% of that seen for WT controls (Figure 10F). In the Morris water maze test, spatial learning of the hidden platform position was acquired similarly in WT and Sez-6 KO animals (Figure 10G). In the probe trial on day 8 after the 7-day training period, however, the preference shown by WT mice for the target quadrant was not exhibited by Sez-6 null mice (Figure 10H), although swim speed and distance traveled did not differ with genotype (not shown). Similar results with respect to lack of preference for the target quadrant were obtained in the probe trial on day 15, although in this trial, Sez-6 null mice did exhibit a reduction in swim speed and distance (not shown).

DISCUSSION

Appropriate dendritic arborization and synapse formation are essential for the production of functional cortical circuitry. Our results provide evidence that Sez-6 proteins are important for specifying proper dendritic arborization and development of excitatory synapses on cortical neurons.

Appropriate Dendritic Branching Requires a Balance of Sez-6 Isoforms

Unlike many factors known to modulate the shape and complexity of dendritic arbors, such as neurotrophins (McAllister et al., 1995), HGF (Gutierrez et al., 2004), Slits (Whitford et al., 2002), and Semaphorins (Fenstermaker et al., 2004), Sez-6 exerted an effect on branching with little discernable effect on overall growth of the arbor, suggesting that these two cellular processes are under independent control. Notch has also been reported to mediate contact-dependent inhibition of dendritic growth while promoting branching (Sestan et al., 1999), providing further evidence that growth and branching are separable processes.

In mouse neurons, the absence of all isoforms of Sez-6 resulted in more highly branched dendritic processes, and a similar effect was seen when neurons of either genotype were treated with the secreted Sez-6 isoform. Overexpression of the membrane-bound isoform, on the other hand, resulted in a simplification of the dendritic arbor, even when branching was stimulated by KCl depolarization. A possible scenario that could explain the ability of secreted Sez-6 to stimulate branching of Sez-6 KO neurons is that membrane-bound Sez-6 blocks a branching signal transduced by another transmembrane protein while secreted Sez-6 competes out this inhibition. The actions of these molecules would then be integrated with those of other factors to specify a physiological pattern of dendritic arborization.

In contrast to the plethora of extracellular factors known to induce branching, far fewer molecules have been reported to inhibit branching, and these function predominantly in intracellular signaling pathways. Intrinsic transcription factors, such as Abrupt and Hamlet, are known to suppress branch formation in particular neuronal subtypes in *Drosophila* embryos (Moore et al., 2002; Sugimura et al., 2004), while RhoA activity transmits anti-branching signals to the cytoskeleton (Van Aelst and Cline, 2004). Neurons expressing the tII isoform alone under both basal and depolarized conditions exhibited fewer neurites, which indicates a role for transmembrane Sez-6 in the suppression of dendritic branching. Recently, a similar action has been reported for the p75 neurotrophin receptor (Zagrebelsky et al., 2005), making these, to our knowledge, the only known vertebrate factors capable of acting at the cell surface to inhibit branching.

Uncoupling of Dendritic Branching and Excitatory Synapse Number in Sez-6 Mutant Cortex

The extent to which synapse formation might regulate or instruct the patterning of dendritic arbors during development remains an open question. The synaptotropic mechanism of dendritic arborization (Vaughn, 1989) has been recently bolstered by real-time imaging studies (Niell et al., 2004; Lohmann et al., 2002); however, other data do not support the synaptotropic hypothesis. For example, although excessive dendritic branching was observed in neurons overexpressing Densin-180, postsynaptic specializations on these branches (labeled with PSD-95) were dramatically reduced (Quitsch et al., 2005). Similarly, we observed increased dendritic branching of cortical neurons lacking Sez-6, and this phenotype was associated with reduced spine numbers, measured by both direct counting and decreased PSD-95 punctate staining. Additionally, our electrophysiological data revealed a reduction in excitatory drive to layer V pyramidal neurons. As there were no changes in the amplitude of spontaneous

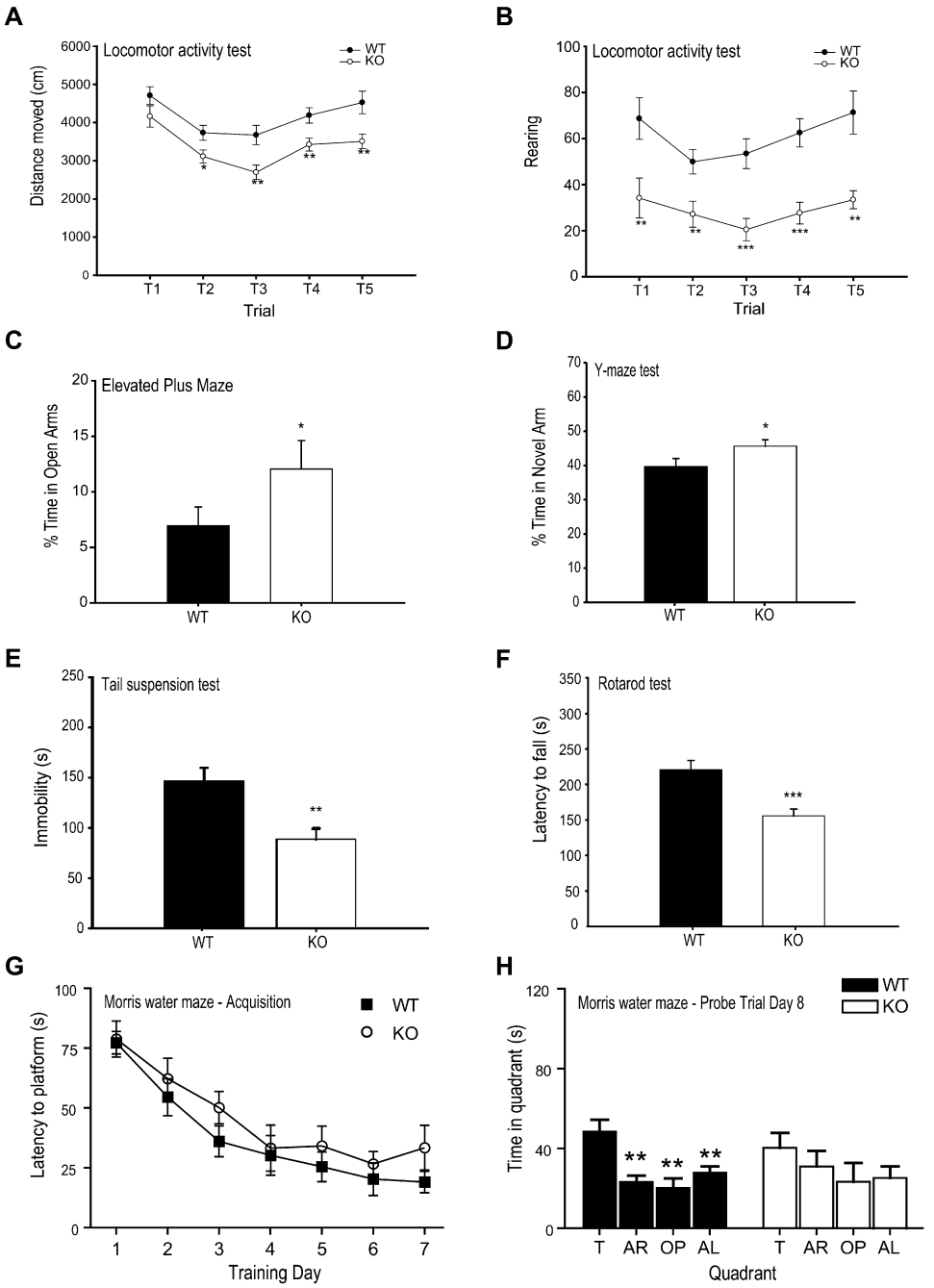

Figure 10. Behavioral Deficits of Sez-6 KO Mice

In the locomotor activity test, Sez-6 null mice (A) covered less distance in the horizontal plane (in trials 2–5 [T2–T5]) and (B) showed fewer entries into the vertical plane (rearings) than Sez-6 WT controls (T1–T5). Sez-6 KO mice spent a greater percentage of time on the open arms of the elevated plus maze (C) and in the novel arm of the Y-maze (D) than Sez-6 WT controls. (E) Tail suspension test: mean time spent immobile (±SEM) over 5 min. Sez-6 KO mice exhibited immobility, indicative of behavioral despair, for shorter periods than WT mice. (F) Rota-Rod test: Sez-6 KO mice displayed a significantly shorter latency to fall than WT mice. (G) Sez-6 KO mice showed no impairment in the acquisition phase of the Morris water maze (days 1–7), but did not display a preference for the target quadrant in probe trials on days 8 (H) and 15 (not shown). *$p < 0.05$; **$p < 0.01$, ***$p < 0.001$.

miniature excitatory synaptic potentials or the response to minimal stimulation, this reduction in excitation is not due to changes in the properties of individual connections but reflects a lower number of excitatory inputs to layer V pyramidal neurons. Thus, in both Sez-6 null and Densin-180-overexpressing neurons, branching appears to be uncoupled from synapse formation or maintenance, arguing against a simple synaptotropic model.

At early developmental stages, the excessive dendritic branching is intrinsic to Sez-6 null mutant neurons and not a contact-dependent phenomenon, since embryonic neurons isolated at E15, prior to the maturation of most synaptic connections and grown under noncontacting conditions, expressed this phenotype. Thus, the reduction in spine number we observed in 5- to 7-week-old mice could represent the outcome of a homeostatic downscaling of active synapses (Turrigiano and Nelson, 2000) to counteract the impact of an initial state of overactivity engendered by excessive branching. Alternatively, since the electrophysiological recordings made in younger (3- to 4-week-old) brains also indicated fewer functional excitatory connections, maintenance of extra branches on layer V pyramidal neurons in the mature *Sez-6*$^{-/-}$ brain could represent a compensatory response to lowered activity in the perinatal period. This latter interpretation is consistent with the finding that blocking synaptic transmission in acute slices led to a 40%–120% increase in the density and length of interstitial filopodial branches on dendritic shafts (but not growth cones) of cortical pyramidal neurons (Portera-Cailliau et al., 2003).

Activity-Dependent Dendritic Branching Is Inhibited by Sez-6 tII Overexpression

Our current data suggest that Sez-6 functions early on in an activity-independent manner but is also capable of modulating activity-dependent dendrite and excitatory synapse development postnatally. Sez-6 is clearly upregulated in response to activity (Shimizu-Nishikawa et al., 1995; Rampon et al., 2000; Håvik et al., 2007) and can alter dendritic arbor patterning induced by activity (as demonstrated in KCl depolarized neurons overexpressing Sez-6 tII). In this context, the idea that Sez-6 could play a role in the development of abnormal wiring in epilepsy is worthy of further investigation. A recent report (Yu et al., 2007) associated Sez-6 mutations (predominantly a truncation mutation that, according to our data, might be predicted to shift the balance in favor of probranching activity) with childhood febrile seizure. This finding is intriguing, although our initial PTZ dose-response data are suggestive of greater resistance to seizure in Sez-6 KO mice, consistent with our findings of reduced excitatory synapse numbers along with unaltered inhibitory inputs.

The precise molecular mechanisms of Sez-6 function are not yet known, although the ability of KCl to robustly increase dendritic branching of Sez-6 KO neurons suggests that activity-dependent branching pathways are intact in the absence of Sez-6. The finding that Sez-6 tII can inhibit activity-dependent dendritic branching induced by KCl, however, indicates that the signaling pathways activated by Sez-6 and those triggered by depolarization can interact. Calcium influx through voltage-gated calcium channels or NMDA receptors triggers activation of several well-characterized pathways, which include the calcium-calmodulin-dependent protein kinase II (CaMKII) pathway, the mitogen-activated protein kinase (MAPK) pathway, and a cascade involving CaMKIV signaling in the nucleus and activation of CREB-stimulated transcription (reviewed by Chen and Ghosh, 2005). Redmond et al. (2002) showed that while stimulation of dendritic branching is mediated by CaMKIV, expression of a constitutively active CaMKII (caCaMKII) dramatically reduced branching. In our overexpression experiments, neurons expressing high levels of Sez-6 tII became quite stunted when stimulated with KCl, a remarkably similar morphological phenotype to that observed with caCaMKII overexpression (Redmond et al., 2002). The possible involvement of CaMKII in signaling downstream of Sez-6 certainly warrants further investigation, particularly since we have recently observed hypophosphorylation of CaMKIIα in Sez-6 KO mouse hippocampus (unpublished data). In addition to transcription-dependent dendritic branching induced by global calcium signals, individual dendritic segments are stabilized locally by neurotransmitter-evoked calcium-induced calcium release, leading to net growth of the dendritic arbor (Lohmann et al., 2002). Since Sez-6 is localized along developing and mature dendritic branches and in dendritic spines, it is well positioned to locally modulate branch stability.

Downstream mechanisms are likely to include an alteration of the balance between the activities of members of the small GTPases Rho, Rac, and cdc42. These molecules are members of key pathways regulating cytoskeletal responses to extracellular signals affecting branching, with Rho acting to oppose branching while Rac and cdc42 act to increase branching of neuronal processes (Van Aelst and Cline, 2004). Similar morphological and electrophysiological changes to those seen in Sez-6 KO mice, namely reduced dendritic length, spine density, and field EPSP amplitude, were observed in mice in which WAVE-1/WRP signaling was disrupted (Soderling et al., 2007). These phenotypic similarities might imply that Sez-6 signals via this complex, which relays signals from Rac to the actin cytoskeleton.

Behavioral Phenotype of Sez-6 Mutant Mice Compounded by Widespread Expression

Sez-6 expression levels are high in the developing cortex; however, postnatally, Sez-6 expression is more marked in other brain regions associated with ongoing morphological plasticity, such as the hippocampus (Figure 1), cerebellum, and olfactory bulb (data not shown). The impaired primary motor ability of Sez-6 KO mice, demonstrated by poor performance on the Rota-Rod, could account for the lower levels of activity in the locomotor cells and very likely involves lack of Sez-6 at extracortical sites, including the granule cells of the cerebellum and neurons of the developing spinal cord. Interestingly, the poor motor coordination demonstrated by Sez-6 null mice on the Rota-Rod did not have demonstrable effects on gait or the withdrawal reflex to a nociceptive stimulus (as measured in the hotplate test). The observation that Sez-6 KO mice spent more time in the open arms of the EPM (despite a similar number of arm entries) could indicate decreased anxiety levels in Sez-6 KO mice (although

this was not apparent in the open field or light/dark tests). This result, together with the reduced immobility in the tail suspension test, indicates that Sez-6 mutant mice behave differently to their WT counterparts under novel, potentially threatening conditions. Interestingly, a similar spectrum of behavioral alterations was reported for WAVE-1 KO mice, which displayed impaired motor coordination and balance, lower activity in the open field, and reduced anxiety, as well as cognitive deficits (Soderling et al., 2003).

In the Morris water maze, no differences between KO mice and controls in latency to platform during learning and acquisition or swimming ability (day 8 probe trial) were observed, indicating that differences in activity levels were not a major confounding factor. Sez-6 mutants did not differ in their ability to acquire the task, although they did fail to display a clear preference for the target quadrant in either probe trial, which is indicative of a long-term memory deficit. Interestingly, Sez-6 has recently been reported to bind neurotrypsin (S. Mitsui et al., 2006, Soc. Neurosci., abstract), a serine protease with important roles in cognition (Molinari et al., 2002) and long-term memory retention (Didelot et al., 2006). Furthermore, specific defects in spatial memory retention similar to those seen in Sez-6 KO mice have recently been reported in mice with disrupted WAVE-1/WRP signaling (Soderling et al., 2007) and in p21-activated kinase dominant-negative (PAKdn) forebrain-specific transgenic mice (Hayashi et al., 2004). PAK is also an important Rac and cdc42 effector, and mutations in PAK-3 cause X-linked mental retardation (Allen et al., 1998). In the case of the PAKdn transgenic mouse, the memory deficit could be attributed to the consolidation phase in the cortex and was accompanied by a reduction in dendritic spine density (although individual synapses were larger; Hayashi et al., 2004). Similarly, WAVE-associated Rac-GTPase activating protein (WRP; also termed MEGAP, or mental disorder-associated GAP) mutations are known to contribute to human 3p(-) syndrome, which includes severe mental retardation (Endris et al., 2002). These phenotypic correlations between mice mutant for Sez-6 or Rac effectors are tantalizing and will no doubt stimulate further investigations into Sez-6 signaling and the role of Sez-6 in cognition.

In conclusion, we have shown that Sez-6 proteins are important for the achievement of the necessary balance between dendrite elongation and branching during the elaboration of a complex dendritic arbor, and for the development of appropriate excitatory synaptic connectivity. The activity-dependent regulation of Sez-6 and its demonstrated ability to modulate activity-dependent dendritic branching are strongly suggestive of a role in the structural plasticity of the maturing brain.

EXPERIMENTAL PROCEDURES

Animal Procedures

All experimental procedures involving animals were approved by the Animal Ethics Committee of the Howard Florey Institute or the University of Queensland. Sez-6 homozygote null and WT same-sex littermate controls were produced by intercross of Sez-6 heterozygote mice (129/SvJ × C57BL/6J background).

Antibody Production and Immunohistochemistry

A cDNA encoding the mouse Sez-6 tIII isoform lacking the native signal peptide (beginning at amino acid Thr27, Shimizu-Nishikawa et al., 1995) was amplified from a SuperscriptII reverse-transcriptase (Invitrogen) -generated template from mouse E15 brain using EXPAND HiFi PCR (Roche). The cDNA was cloned in-frame into the NheI/NotI restricted CMV-N-FLAG vector (Tunggal et al., 2003) and sequence verified. The amino terminal FLAG epitope-tagged recombinant Sez-6 tIII protein was purified from transfected Cos-7 cell-conditioned medium on an anti-FLAG affinity resin and used to produce a rabbit polyclonal anti-Sez-6 antiserum. A 1/1000 dilution (3rd bleed) was used on 14 μm cryostat sections of 4% paraformaldehyde (PFA) fixed tissue. Details of other primary and secondary antibodies and PSD-95 staining are supplied in Supplemental Methods.

Subcellular Fractionation and Western Blot

Synaptosomes were prepared as described (Srivastava et al., 1998) and further fractionated (Phillips et al., 2001). Material in the postsynaptic fraction not solubilized by 5% SDS was taken up in 8M urea (to a total volume of 60 μl). Tissue protein extracts in RIPA buffer with protease inhibitors (Complete Mini; Roche Diagnostics) or protein fractions were resolved using SDS-PAGE and transferred to BioTrace PVDF membranes (Pall Corporation, Port Washington, NY). Primary antibodies were rabbit α-Sez-6 (in house; 1/1000), rabbit α-PSD-95 (Zymed, South San Francisco, CA; 1/1500), mouse α-synaptophysin (Clone SVP-38, Sigma, Australia; 1/3000) and mouse α-beta actin (Sigma, Australia; 1/5000). The secondary antibody was either horseradish peroxidase (HRP)-conjugated sheep anti-rabbit Ig (Silenus, VIC, Australia; 1/4000) or HRP-conjugated goat anti-mouse IgG (Upstate, Charlottesville, VA; 1/20,000).

Sez-6 Null Mutant Mice

Refer to Supplemental Methods.

Primary Neuron Culture

Cortices from WT or Sez-6 KO embryos (E15.5; see Supplemental Methods for genotyping) were pooled separately and tissue was digested with the Papain Dissociation Kit (Worthington Biochemical Corporation, Lakewood, NJ). For low-density cultures, neurons were plated at 1–5 × 10^4/ml on poly-DL-ornithine/laminin-coated coverslips in Neurobasal medium + 2% B27 supplement (Invitrogen, VIC, Australia), 0.5 mM glutamine, and antibiotics (50 IU/ml penicillin, 50 μg/ml streptomycin). For feeder-layer experiments, primary neurons were plated on Cos-7 cells secreting Sez-6 tIII or control cells with episomally maintained empty N-FLAG vector. Sez-6 tIII conditioned medium (2–3 days) was diluted 1:1 with complete Neurobasal medium for plating and replacement of conditioned medium on day 2 of culture. For scoring neurite parameters, neurons cultured for 2–5 days were stained with mouse anti-β-III tubulin (TuJ1, Covance, Richmond, CA; 1/500 dilution). Duplicate coverslips (or wells, for neurons on feeder layers) were scored for each condition. For E15 WT and KO cultures, only neurons lacking contacts with other neurons were scored. For E17 WT cultures treated with Sez-6 tIII conditioned medium, neurons contacting other neurons were scored. Data from two independent experiments were combined.

For transfection of primary E15 neurons, the Amaxa nucleofection system was utilized (Amaxa, Germany). Transfections were carried out using the Program O-005 for mouse hippocampal neurons with combined expression constructs for Sez-6 isoforms and Venus EYFP (Nagai et al., 2002) in a molar ratio of 3:1. Neurons were plated in Neurobasal medium, except for neurons to be treated with KCl, which were plated in Amaxa medium I (90% DMEM + 10% heat-inactivated FCS) and, after 3–4 hr, changed into Neurobasal medium (as

above) containing 5% heat-inactivated FCS. KCl (50 mM) was added at 3 DIV for 24 hr before neurons were fixed (4% PFA, 3 min) for immunostaining.

Dendritic spines on TRITC-phalloidin (Sigma, Australia; 1/100 of 50 μg/ml stock in EtOH) -stained cortical neurons (14 DIV) were scored on dendritic segments (40 μm) proximal to the soma. All protrusions less than 5 μm in length were counted and the presence or absence of a head region wider than the neck was recorded. For each genotype, 60 dendritic segments were scored.

Golgi-Cox Impregnation

Modified Golgi-Cox impregnation of neurons was performed using the FD RapidGolgi Stain kit (FD NeuroTechnologies, Ellicot City, MD). Brains (five pairs of WT and KO same-sex littermates) from 5- to 7-week-old mice were fixed, sectioned, and developed in parallel. For dendritic analyses, camera lucida drawings of 30 layer V/VI pyramidal neurons per genotype from 50 μm sections were made.

Spines were counted in 150 μm sections. Dendritic segments (50 μm) extending proximally from distal tips (or sites of truncation) toward the primary apical dendrite of layer V pyramidal neurons were scored if the proximal end of the segment lay at least 50 μm into layer II/III. Aspinous neurons were excluded for spine counts and, for all Golgi-Cox analyses, only neurons of the somatosensory cortex were considered. Confocal images of spines were made using a Zeiss LSM5 Pascal microscope with 63× magnification and 2.2× digital zoom.

Electrophysiology

Details of slice preparation are supplied in Supplemental Methods. Whole-cell recordings were made from layer V pyramidal neurons in the somatosensory cortex using IR/DIC techniques. Electrodes (3–5 MΩ) were filled with pipette solution containing 135 mM $KMeSO_4$, 8 mM NaCl, 10 HEPES, 2 mM Mg_2ATP, 0.3 mM Na_3GTP, and 0.3 mM EGTA (pH 7.2 with KOH, osmolarity 300 mOsm/kg). For voltage-clamp recordings $KMeSO_4$ was replaced with $CsMeSO_4$, and 0.1 mM spermine was added. Signals were recorded using a patch-clamp amplifier (Multiclamp 700A, Axon instruments, Foster City, CA). Responses were filtered at 4–8 kHz and digitized at 10 kHz (Instrutech, Greatneck, NY, USA, ITC-16). All data were acquired, stored, and analyzed on a Macintosh G4 using Axograph (Axon Instruments). Only cells with a membrane potential greater than −55 mV were included in this study. Access resistance was 5–20 MΩ and was monitored throughout the experiment by periodically balancing the bridge during current-clamp recordings. To investigate the firing properties of neurons, prolonged current injection steps (600 ms) were applied from −100 pA to +600 pA in 50 pA increments. Threshold was taken as the current injection that first evoked action potential firing. Synaptic responses were evoked by injecting 0.05 ms constant current pulses into layer II/III somatosensory cortex using a theta glass stimulator. EPSPs are averages of ten sweeps. Input-output relationships were examined by measuring the amplitude of EPSPs evoked by increasing stimulus intensities between 1V and 100V. The spike initiation threshold for action potentials evoked on EPSPs was measured at the membrane potential just before the upstroke of the action potential. mEPSCs were recorded in voltage-clamp in the presence of 1 μM TTX for 5 min at a sampling rate of 20 kHz. The frequency of mEPSCs was ~0.4 Hz in neurons of either genotype, and the number of mEPSCs analyzed per neuron ranged between 12 and 278. Minimal stimulation-evoked synaptic responses were examined in voltage-clamp. A minimal stimulating intensity was used to evoke EPSCs at an intensity where failures occurred at least 4% of the time. An average of up to 50 sweeps was taken after exclusion of the failed EPSCs. Results are expressed as mean ± SEM.

Behavioral Analyses

Refer to Supplemental Methods.

Image Analysis and Statistics

Images of neurons were captured using a digital SPOT camera. Neurons were traced and their parameters were measured using ImagePro Plus by an investigator blinded to the experimental condition. Integrated pixel density in a 200 μm^2 region of interest (ROI) of PSD-95-immunostained neuropil was determined using NIH ImageJ. Pairwise comparisons were tested for significance using two-tailed Student's t test. For analyses of nonnormally distributed data (normality tested using the Kolmogorov-Smirnoff test), the nonparametric tests Mann-Whitney Rank Sum test or Kruskal-Wallis ANOVA on Ranks were used. Tests which returned $p < 0.05$ were considered significant.

Supplemental Data

The Supplemental Data for this article can be found online at http://www.neuron.org/cgi/content/full/56/4/621/DC1/.

ACKNOWLEDGMENTS

We thank Neil Smyth and Olan Dolezal for reagents; Kylie Shipham, Frank Weissenborn, and Arena Yao for excellent technical assistance; Fiona Christensen for microinjection of embryonic stem cells; Rian Mackenzie, Lisa Bray, and Krista Brown for mouse colony maintenance; Rachel Nally, Keith Buxton, Brett Purcell, and Maarten van den Buuse of the Integrative Neuroscience Facility, Howard Florey Institute for behavioral testing and analysis; and Anthony Hannan for helpful discussions. This work was supported by Project Grant 454462 from the National Health and Medical Research Council, Australia and a Neurosciences Victoria / Centre for Neuroscience Fellowship (to J.M.G.). The authors declare that they have no competing financial interests.

Received: May 9, 2006
Revised: January 25, 2007
Accepted: September 11, 2007
Published: November 20, 2007

REFERENCES

Allen, K.M., Gleeson, J.G., Bagrodia, S., Partington, M.W., MacMillan, J.C., Cerione, R.A., Mulley, J.C., and Walsh, C.A. (1998). PAK3 mutation in nonsyndromic X-linked mental retardation. Nat. Genet. *20*, 25–30.

Bading, H., Ginty, D.D., and Greenberg, M.E. (1993). Regulation of gene expression in hippocampal neurons by distinct calcium signaling pathways. Science *260*, 181–186.

Chen, Y., and Ghosh, A. (2005). Regulation of dendritic development by neuronal activity. J. Neurobiol. *64*, 4–10.

Chklovskii, D.B., Mel, B.W., and Svoboda, K. (2004). Cortical rewiring and information storage. Nature *431*, 782–788.

Didelot, G., Molinari, F., Tchénio, P., Comas, D., Milhiet, E., Munnich, A., Colleaux, L., and Preat, T. (2006). Tequila, a neurotrypsin ortholog, regulates long-term memory formation in *Drosophila*. Science *313*, 851–853.

Endris, V., Wogatzky, B., Leimer, U., Bartsch, D., Zatyka, M., Latif, F., Maher, E.R., Tariverdian, G., Kirsch, S., Karch, D., and Rappold, G.A. (2002). The novel Rho-GTPase activating gene MEGAP/srGAP3 has a putative role in severe mental retardation. Proc. Natl. Acad. Sci. USA *99*, 11754–11759.

Fenstermaker, V., Chen, Y., Ghosh, A., and Yuste, R. (2004). Regulation of dendritic length and branching by semaphorin 3A. J. Neurobiol. *58*, 403–412.

Gally, C., Eimer, S., Richmond, J.E., and Bessereau, J.-L. (2004). A trans-membrane protein required for acetylcholine receptor clustering in Caenorhabditis elegans. Nature *431*, 578–582.

Glantz, L.A., and Lewis, D.A. (2000). Decreased dendritic spine density on prefrontal cortical pyramidal neurons in schizophrenia. Arch. Gen. Psychiatry *57*, 65–73.

Goldshmit, Y., Greenhalgh, C.J., and Turnley, A.M. (2004). Suppressor of cytokine signalling-2 and epidermal growth factor regulate neurite outgrowth of cortical neurons. Eur. J. Neurosci. *20*, 2260–2266.

Gunnersen, J.M., Augustine, C., Spirkoska, V., Kim, M., Brown, M., and Tan, S.-S. (2002). Global analysis of gene expression patterns in developing mouse neocortex using serial analysis of gene expression. Mol. Cell. Neurosci. *19*, 560–573.

Gutierrez, H., Dolcet, X., Tolcos, M., and Davies, A. (2004). HGF regulates the development of cortical pyramidal dendrites. Development *131*, 3717–3726.

Haas, K., Li, J., and Cline, H.T. (2006). AMPA receptors regulate experience-dependent dendritic arbor growth in vivo. Proc. Natl. Acad. Sci. USA *103*, 12127–12131.

Häusser, M., Spruston, N., and Stuart, G.J. (2000). Diversity and dynamics of dendritic signaling. Science *290*, 739–744.

Håvik, B., Røkke, H., Dagyte, G., Stavrum, A.K., Bramham, C.R., and Steen, V.M. (2007). Synaptic activity-induced global gene expression patterns in the dentate gyrus of adult behaving rats: induction of immunity-linked genes. Neuroscience *148*, 925–936.

Hayashi, M.L., Choi, S.Y., Shankaranarayana Rao, B.S., Jung, H.-Y., Lee, H.-K., Zhang, D., Chattarji, S., Kirkwood, A., and Tonegawa, S. (2004). Altered cortical synaptic morphology and impaired memory consolidation in forebrain-specific dominant-negative PAK transgenic mice. Neuron *42*, 773–787.

Kim, M.H., Gunnersen, J.M., and Tan, S.-S. (2002). Localized expression of the seizure-related gene SEZ-6 in developing and adult forebrains. Mech. Dev. *118*, 171–174.

Lohmann, C., Myhr, K.L., and Wong, R.O.L. (2002). Transmitter-evoked local calcium release stabilizes developing dendrites. Nature *418*, 177–181.

Marín, O., Yaron, A., Bagri, A., Tessier-Lavigne, M., and Rubenstein, J.L.R. (2001). Sorting of striatal and cortical interneurons regulated by semaphorin-neuropilin interactions. Science *293*, 872–875.

McAllister, A.K., Lo, D.C., and Katz, L.C. (1995). Neurotrophins regulate dendritic growth in developing visual cortex. Neuron *15*, 791–803.

Molinari, F., Rio, M., Meskenaite, V., Encha-Razavi, F., Augé, J., Bacq, D., Briault, S., Vekemans, M., Munnich, A., Attié-Bitach, T., et al. (2002). Truncating neurotrypsin mutation in autosomal recessive nonsyndromic mental retardation. Science *298*, 1779–1781.

Moore, A.W., Jan, L.Y., and Jan, Y.N. (2002). hamlet, a binary genetic switch between single- and multiple-dendrite neuron morphology. Science *297*, 1355–1358.

Nagai, T., Ibata, K., Park, E.S., Kubota, M., Mikoshiba, K., and Miyawaki, A. (2002). A variant of yellow fluorescent protein with fast and efficient maturation for cell-biological applications. Nat. Biotechnol. *20*, 87–90.

Niblock, M.M., Brunso-Bechtold, J.K., and Riddle, D.R. (2000). Insulin-like growth factor I stimulates dendritic growth in primary somatosensory cortex. J. Neurosci. *20*, 4165–4176.

Niell, C.M., Meyer, M.P., and Smith, S.J. (2004). In vivo imaging of synapse formation on a growing dendritic arbour. Nat. Neurosci. *7*, 254–260.

Phillips, G.R., Huang, J.K., Wang, Y., Tanaka, H., Shapiro, L., Zhang, W., Shan, W.S., Arndt, K., Frank, M., Gordon, R.E., et al. (2001). The pre-synaptic particle web: ultrastructure, composition, dissolution, and reconstitution. Neuron *32*, 63–77.

Polleux, F., Morrrow, T., and Ghosh, A. (2000). Semaphorin 3A is a chemoattractant for cortical apical dendrites. Nature *404*, 567–573.

Portera-Cailliau, C., Pan, D.T., and Yuste, R. (2003). Activity-regulated dynamic behaviour of early dendritic protrusions: evidence for different types of dendritic filopodia. J. Neurosci. *23*, 7129–7142.

Quitsch, A., Berhörster, K., Liew, C.W., Richter, D., and Kreienkamp, H.-J. (2005). Post-synaptic shank antagonizes dendrite branching induced by the leucine-rich repeat protein Densin-180. J. Neurosci. *25*, 479–487.

Raastad, M., Storm, J.F., and Andersen, P. (1992). Putative single quantum and single fiber excitatory postsynaptic currents show similar amplitude range and variability in rat hippocampal slices. Eur. J. Neurosci. *4*, 113–117.

Rampon, C., Jiang, C.H., Dong, H., Tang, Y.P., Lockhart, D.J., Schultz, P.G., Tsien, J.Z., and Hu, Y. (2000). Effects of environmental enrichment on gene expression in the brain. Proc. Natl. Acad. Sci. USA *97*, 12880–12884.

Redmond, L., Kashani, A.H., and Ghosh, A. (2002). Calcium regulation of dendritic growth via CaM kinase IV and CREB-mediated transcription. Neuron *34*, 999–1010.

Riccio, R.V., and Matthews, M.A. (1985). Effects of intraocular tetrodotoxin on dendritic spines in the developing rat visual cortex: a Golgi analysis. Brain Res. *351*, 173–182.

Sahay, A., Kim, C.-H., Sepkuty, J.P., Cho, E., Huganir, R.L., Ginty, D.D., and Kolodkin, A.L. (2005). Secreted semaphorins modulate synaptic transmission in the adult hippocampus. J. Neurosci. *25*, 3613–3620.

Sestan, N., Artavanis-Tsakonas, S., and Rakic, P. (1999). Contact-dependent inhibition of cortical neurite growth mediated by notch signaling. Science *286*, 741–746.

Shimizu-Nishikawa, K., Kajiwara, K., Kimura, M., Katsuki, M., and Sugaya, E. (1995). Cloning and expression of SEZ-6, a brain-specific and seizure-related cDNA. Brain Res. Mol. Brain Res. *28*, 201–210.

Soderling, S.H., Langeberg, L.K., Soderling, J.A., Davee, S.M., Simerly, R., Raber, J., and Scott, J.D. (2003). Loss of WAVE-1 causes sensorimotor retardation and reduced learning and memory in mice. Proc. Natl. Acad. Sci. USA *100*, 1723–1728.

Soderling, S.H., Guire, E.S., Kaech, S., White, J., Zhang, F., Schutz, K., Langeberg, L.K., Banker, G., Raber, J., and Scott, J.D. (2007). A WAVE-1/WRP signaling complex regulates spine density, synaptic plasticity and memory. J. Neurosci. *27*, 355–365.

Srivastava, S., Osten, P., Vilim, F.S., Khatri, L., Inman, G., States, B., Daly, C., De Souza, S., Abagyan, R., Valtschanoff, J.G., et al. (1998). Novel anchorage of GluR2/3 to the postsynaptic density by the AMPA receptor-binding protein ABP. Neuron *21*, 581–591.

Suetsugu, M., and Mehraein, P. (1980). Spine distribution along the apical dendrites of the pyramidal neurons in Down's syndrome. A quantitative Golgi study. Acta Neuropathol. (Berl.) *50*, 207–210.

Sugimura, K., Satoh, D., Estes, P., Crews, S., and Uemura, T. (2004). Development of morphological diversity of dendrites in Drosophila by the BTB-zinc finger protein Abrupt. Neuron *43*, 809–822.

Swann, J.W., Al-Noori, S., Jiang, M., and Lee, C.L. (2000). Spine loss and other dendritic abnormalities in epilepsy. Hippocampus *10*, 617–625.

Tailby, C., Wright, L.L., Metha, A.B., and Calford, M.B. (2005). Activity-dependent maintenance and growth of dendrites in adult cortex. Proc. Natl. Acad. Sci. USA *102*, 4631–4636.

Trachtenberg, J.T., Chen, B.E., Knott, G.W., Feng, G., Sanes, J.R., Welker, E., and Svoboda, K. (2002). Long-term in vivo imaging of experience-dependent synaptic plasticity in the adult cortex. Nature *420*, 788–794.

Tunggal, J., Wartenberg, M., Paulsson, M., and Smyth, N. (2003). Expression of the nidogen-binding site of the laminin 1 chain disturbs basement membrane formation and maintenance in F9 embryoid bodies. J. Cell Sci. *116*, 803–812.

Turrigiano, G.G., and Nelson, S.B. (2000). Hebb and homeostasis in neuronal plasticity. Curr. Opin. Neurobiol. *10*, 358–364.

Van Aelst, L., and Cline, H.T. (2004). Rho GTPases and activity-dependent dendrite development. Curr. Opin. Neurobiol. *14*, 297–304.

Vaughn, J.E. (1989). Fine structure of synaptogenesis in the vertebrate central nervous system. Synapse *3*, 255–285.

Wakana, S., Sugaya, E., Naramoto, F., Yokote, N., Maruyama, C., Jin, W., Ohguchi, H., Tsuda, T., Sugaya, A., and Kajiwara, K. (2000). Gene mapping of SEZ group genes and determination of pentylenetetrazol susceptible quantitative trait loci in the mouse chromosome. Brain Res. *857*, 286–290.

Whitford, K.L., Marillat, V., Stein, E., Goodman, C.S., Tessier-Lavigne, M., Chédotal, A., and Ghosh, A. (2002). Regulation of cortical dendrite development by Slit-Robo interactions. Neuron *33*, 47–61.

Williams, S.R., and Stuart, G.J. (1999). Mechanisms and consequences of action potential burst firing in rat neocortical pyramidal neurons. J. Physiol. *521*, 467–482.

Wong, R.O.L., and Ghosh, A. (2002). Activity-dependent regulation of dendritic growth and patterning. Nat. Rev. Neurosci. *3*, 803–812.

Wu, G.Y., Zou, D.J., Rajan, I., and Cline, H. (1999). Dendritic dynamics in vivo change during neuronal maturation. J. Neurosci. *19*, 4472–4483.

Yu, Z., Jiang, J., Wu, D., Xie, H., Jiang, J., Zhou, L., Peng, L., and Bao, G. (2007). Febrile seizures are associated with mutation of seizure-related (SEZ) 6, a brain-specific gene. J. Neurosci. Res. *85*, 166–172.

Zagrebelsky, M., Holz, A., Dechant, G., Barde, Y.-A., Bonhoeffer, T., and Korte, M. (2005). The p75 neurotrophin receptor negatively modulates dendrite complexity and spine density in hippocampal neurons. J. Neurosci. *25*, 9989–9999.

Zheng, Y., Mellem, J.E., Brockie, P.J., Madsen, D.M., and Maricq, A.V. (2004). SOL1 is a CUB-domain protein required for GLR-1 glutamate receptor function in C. elegans. Nature *427*, 451–457.